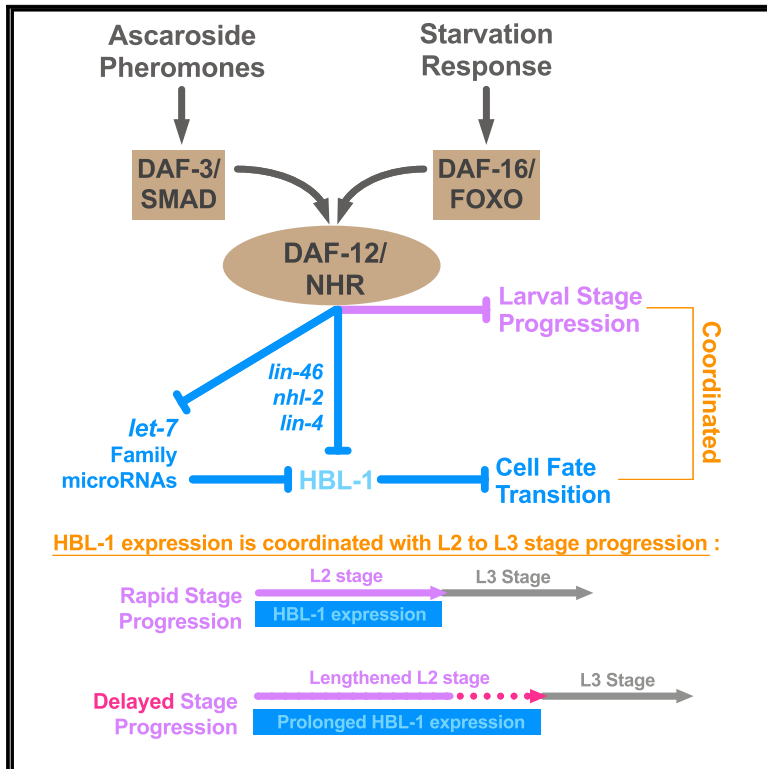


Current Biology

Pheromones and Nutritional Signals Regulate the Developmental Reliance on *let-7* Family MicroRNAs in *C. elegans*

Graphical Abstract



Authors

Orkan Ilbay, Victor Ambros

Correspondence

victor.ambros@umassmed.edu

In Brief

Ilbay and Ambros show that pheromones and nutritional signals coordinately regulate developmental progression and cell-fate transitions during *C. elegans* development, and this coordination involves activation of an alternative temporal downregulation program for a critical *let-7* family target, HBL-1.

Highlights

- Ascr#5 corrects heterochronic cell-fate defects of *daf-12(rh61)* mutants
- Ascarosides reduce the developmental reliance on *let-7* family microRNAs
- DAF-12 mediates an L2d rewiring of networks controlling temporal cell fates
- Developmental progression and temporal cell fates are coordinately regulated



Pheromones and Nutritional Signals Regulate the Developmental Reliance on *let-7* Family MicroRNAs in *C. elegans*

Orkan Ilbay¹ and Victor Ambros^{1,2,*}¹Program in Molecular Medicine, University of Massachusetts Medical School, 373 Plantation Street, Worcester, MA 01605, USA²Lead Contact*Correspondence: victor.ambros@umassmed.edu<https://doi.org/10.1016/j.cub.2019.04.034>

SUMMARY

Adverse environmental conditions can affect rates of animal developmental progression and lead to temporary developmental quiescence (diapause), exemplified by the dauer larva stage of the nematode *Caenorhabditis elegans* (*C. elegans*). Remarkably, patterns of cell division and temporal cell-fate progression in *C. elegans* larvae are not affected by changes in developmental trajectory. However, the underlying physiological and gene regulatory mechanisms that ensure robust developmental patterning despite substantial plasticity in developmental progression are largely unknown. Here, we report that diapause-inducing pheromones correct heterochronic developmental cell lineage defects caused by insufficient expression of *let-7* family microRNAs in *C. elegans*. Moreover, two conserved endocrine signaling pathways, DAF-7/TGF- β and DAF-2/Insulin, that confer on the larva diapause and non-diapause alternative developmental trajectories interact with the nuclear hormone receptor, DAF-12, to initiate and regulate a rewiring of the genetic circuitry controlling temporal cell fates. This rewiring includes engagement of certain heterochronic genes, *lin-46*, *lin-4*, and *nhl-2*, that are previously associated with an altered genetic program in post-diapause animals, in combination with a novel ligand-independent DAF-12 activity, to downregulate the critical *let-7* family target Hunchback-like-1 (HBL-1). Our results show how pheromone or endocrine signaling pathways can coordinately regulate both developmental progression and cell-fate transitions in *C. elegans* larvae under stress so that the developmental schedule of cell fates remains unaffected by changes in developmental trajectory.

INTRODUCTION

Despite the vast complexity of animal development, developmental processes are remarkably robust in the face of environment and physiological stresses. Multicellular animals develop

from a single cell through a temporal and spatial elaboration of events that include cell division, differentiation, migration, and apoptosis. Early developmental cell lineages rapidly diverge functionally and spatially and continue to follow distinct paths toward building diverse parts of the animal body. Marvelously, the sequence and synchrony of these increasingly complex programs of cell-fate progression are precisely coordinated, regardless of various environmental and physiological stresses that the animal may encounter in its natural environment.

The nematode *C. elegans* develops through four larval stages, each of which consists of an invariant set of characteristic developmental events [1]. During larval development, stem cells and blast cells divide and progressively produce progeny cells with defined stage-specific fates. The timing of cell-fate transitions within individual postembryonic cell lineages is regulated by genes of the heterochronic pathway, whose products include cell-fate-determinant transcription factors as well as microRNAs (miRNAs) and other regulators of these transcription factors [2, 3]. In mutants defective in the activity of one or more heterochronic genes, the synchrony between cell fates and developmental stages is lost in certain cell lineages, which results in dissonance in the relative timing of developmental events across the animal and consequently morphological abnormalities.

During *C. elegans* larval development, lateral hypodermal stem cells (“seam cells”) express stage-specific proliferative or self-renewal behavior (Figure 1A). Particularly, while seam cells divide asymmetrically at each larval stage (L1–L4), giving rise to a new seam cell and a differentiating hypodermal (hyp7) cell, at the L2 stage, certain seam cells also undergo a single round of symmetric cell division, resulting in an increase in the number of seam cells on each side of the animal from ten to sixteen. This L2-specific proliferative cell fate is driven by a transcription factor, HBL-1, which specifies expression of the L2 cell fate and also prevents the expression of the L3 cell fates [4, 5]. Therefore, in order to allow progression to L3 cell fates, HBL-1 must be downregulated by the end of the L2 stage. If HBL-1 is not properly downregulated, for example in mutants defective in upstream regulatory genes, seam cells inappropriately execute L2 cell fates at later stages, resulting in an enlarged and developmentally retarded population of seam cells in adult worms. Three *let-7* family miRNAs (*mir-48*, *mir-84*, and *mir-241*) are redundantly required for proper temporal downregulation of HBL-1 [6]. Larvae lacking all three *let-7* family miRNAs reiterate L2 cell fates in later stages of development. The degree of reiteration, hence the severity of the phenotype, varies depending on



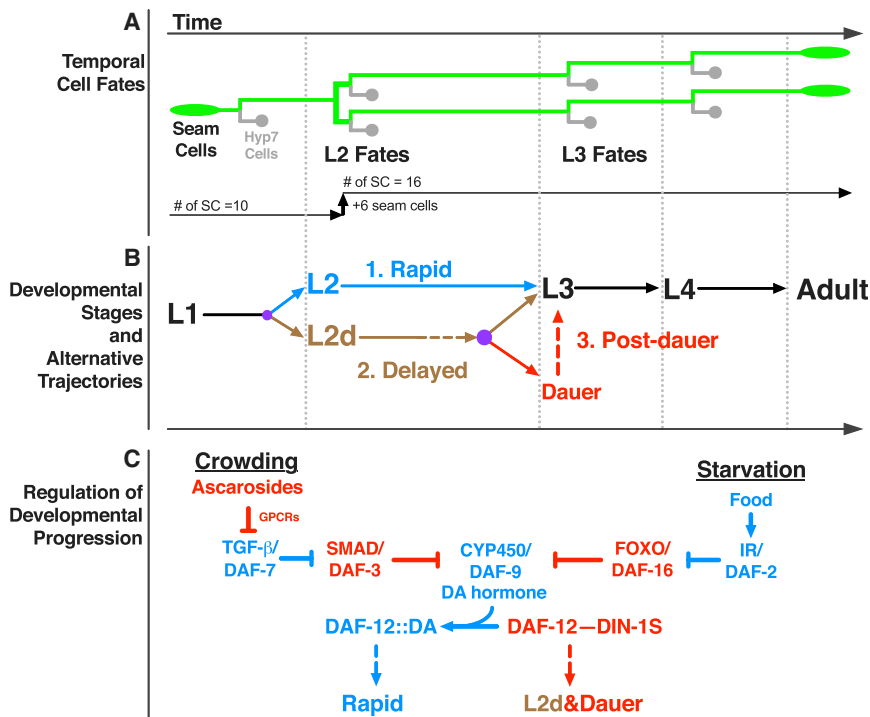


Figure 1. Temporal Fates of Hypodermal Seam Cells Are Robust against Changes in Developmental Trajectory Induced by Crowding or Starvation

(A) Lineage diagram showing temporal (stage-specific) hypodermal seam cell fates. Seam cells (green) divide asymmetrically at each larval stage, renewing themselves while giving rise to hyp7 cells (gray). At the L2 stage, seam cells undergo a single round of symmetric cell division, resulting in an increase in their number. Note that only six out of ten seam cells undergo symmetric cell division, which increases the total number of seam cells on each side of the worm from ten to sixteen.

(B) Developmental stages and three distinct developmental trajectories: (1) continuous, unipotent, and rapid progression define the L2 trajectory (blue); (2) continuous but bipotent and delayed progression define the L2d trajectory (brown); and (3) developmental progression is interrupted by a diapause in the dauer-interrupted trajectory (brown followed by red). The time axis indicates the order of events in time (not proportional to absolute time). Vertical dotted lines indicate the molts between stages. Purple dots represent decision points between different trajectory options.

(C) Regulation of developmental progression. Under favorable conditions, dafachronic acid (DA) hormone is abundant, and DA-bound DAF-12

promotes rapid development. Crowding or starvation induces L2d and dauer formation by repressing TGF- β /DAF-7 signals or insulin signaling (IR/DAF-2: insulin receptor), respectively. Activated effectors of these signaling pathways (DAF-3 or DAF-16) inhibit the biosynthesis of DA, and the unliganded DAF-12 interacts with DIN-1S, which together promote L2d and dauer formation.

genetic and environmental factors [7] and can be quantified by counting the number of seam cells in young adult worms.

C. elegans is a free-living nematode whose environment is prone to fluctuations between conditions that are favorable and unfavorable for completion of development [8]. Under favorable conditions (such as abundant food), *C. elegans* larvae develop rapidly and continuously progress through the four larval stages to the adult (Figure 1B, rapid). However, when the conditions are not favorable (for example, in the face of declining resources owing to high population density), the larva at the end of the L2 stage can elect to enter a developmentally arrested diapause, called the dauer larva, which is non-feeding, stress resistant, and long lived [9]. When conditions improve, the dauer larva resumes development to the reproductive adult (Figure 1B, post-dauer). The DAF-7/TGF- β and DAF-2/insulin endocrine signaling pathways are the two major signaling pathways that regulate *C. elegans* dauer larva diapause. These two pathways act in parallel to integrate information about population density and nutritional status by co-modulating the biosynthesis of the dafachronic acid (DA) hormone. DA is the ligand of a nuclear hormone receptor, DAF-12, which opposes dauer formation when it is DA-bound and forms a repressor complex with DIN-1S and promotes dauer formation when it is unliganded (Figure 1C) [10].

The order and sequence of temporal cell fates in the various *C. elegans* larval cell lineages are robustly maintained regardless of developmental trajectory: for example, blast cells properly transition from L2 to L3 fates whether the larva develops rapidly and continuously or instead traverses dauer diapause, which imposes a lengthy (even months-long) interruption of the L2 to L3

transition (Figures 1A and 1B). Interestingly, cell-fate transition defects of many heterochronic mutants are modified (either suppressed or enhanced) when larval development is interrupted by dauer diapause, suggesting that the genetic regulatory pathways regulating temporal cell-fate progression are modified depending on whether the animal develops continuously versus undergoes dauer-interrupted development [11–13]. The mechanisms by which temporal cell-fate specification pathways are modified in association with the dauer larva trajectory are poorly understood, especially with regards to how modifications to the regulatory networks controlling temporal cell-fate transitions may be coupled to particular steps in the specification and/or execution of the dauer larva diapause trajectory. Of particular interest is the question of whether and how the dauer-promoting signals that are monitored by L1 and L2d larvae might act prior to dauer commitment to directly modify gene regulatory mechanisms controlling temporal cell-fate transitions.

To investigate the impact of dauer-inducing environmental and endocrine signals on the regulatory network controlling temporal cell-fate transitions, we employed experimental conditions that not only induce the dauer formation program but also efficiently prevent dauer commitment. We call these conditions “L2d inducing” because the presence of both dauer-inducing and commitment-preventing conditions results in worm populations growing continuously (without dauer arrest) but where all animals traverse the lengthened bi-potential L2d stage (Figure 1B, L2d/delayed) [14, 15].

We found that L2d-inducing pheromones suppress heterochronic defects caused by insufficient expression of *let-7* family

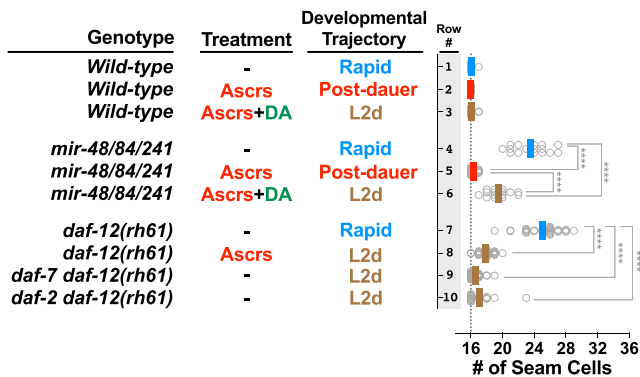


Figure 2. Sensitized Genetic Backgrounds Reveal that L2d-Inducing Environmental and Endocrine Signals Impact the Regulation of Temporal Cell Fates

Genotypes are indicated in the first column; treatments and corresponding developmental trajectories are indicated in the second and third columns, respectively. Each dot in the plots to the right shows the number of seam cells on one side (left side or right side, observed interchangeably) of a single young adult animal, and solid lines (color code matching the developmental trajectory) indicate the average seam cell number of the animals scored for each condition. Wild-type animals have sixteen seam cells per side (vertical dotted line), regardless of developmental trajectory (lines 1–3). Experiments involving temperature-sensitive alleles of *daf-2* and *daf-7* (lines 9 and 10) are performed at a permissive temperature (20° C) that allows continuous (L2d-to-L3 without dauer arrest) development. The Student's *t* test is used to calculate statistical significance (p): n.s. (not significant) $p > 0.05$, * $p < 0.05$, ** $p < 0.01$, *** $p < 0.001$, **** $p < 0.0001$. See also Figure S1 and S2 and Table S1.

microRNAs, suggesting that these pheromones that enable the dauer life history option also activate a program alternative to *let-7* family microRNAs in controlling stage-specific temporal cell-fate progression. We found that the two major endocrine signaling pathways that regulate dauer formation in response to pheromones and food signals, the DAF-7/TGF- β and DAF-2/Insulin, respectively, also mediate the effect of these same signals on temporal cell fates under L2d-inducing conditions. Moreover, we identified a previously undescribed ligand-independent activity of the nuclear hormone receptor DAF-12 that is responsible for activating the alternative program of cell-fate specification in the L2d. This alternative program is responsible for correcting *let-7* family insufficiency phenotypes, and it requires the activities of certain heterochronic genes, *lin-46*, *lin-4*, and *nhl-2*, that are previously associated with an altered genetic program in post-diapause animals. This alternative program associated with L2d is coupled to a previously described reduction in the DAF-12-regulated expression of *let-7* family microRNAs [16]. Hence, the overall L2d response is a “rewiring” program consisting two major operations: (1) repression of *let-7* family microRNA expression, and (2) activation of an alternative program to downregulate the *let-7* family target (Hunchback-like-1) HBL-1.

Our results show that environmental signals and downstream endocrine signaling pathways are capable of coordinately regulating developmental progression and cell-fate transitions in *C. elegans*. We propose that this capability confers elasticity to *C. elegans* development, whereby the proper developmental schedule of cell fates remains unaffected by changes or uncertainties in developmental trajectory.

RESULTS

We developed three approaches to efficiently uncouple L2d from dauer commitment and thereby produce worm populations developing continuously through the bi-potential pre-dauer L2d phase directly to the L3, without dauer arrest. In the first approach, we employed the pheromone cocktail formula described by Butcher et al. [17], which contains three ascaroside molecules (*ascr#2*, *ascr#3*, and *ascr#5*) that synergistically induce L2d and dauer arrest [17] (Figure S1A). At sufficiently high doses, the ascaroside cocktail can induce 100% dauer formation (Figure S1C). Previous findings showed that the presence of food can antagonize pheromones and prevent dauer formation [14]. However, it was not clear if the food signals also prevented the L2d. We observed that the presence of live bacteria food, or the presence of dafachronic acid (DA) hormone, could efficiently prevent dauer formation while not preventing the L2d, evidenced by dramatically slowed second-stage larval development. Therefore, to obtain animal populations traversing the L2d without committing to dauer arrest, we allowed larvae to develop in the presence of a combination of the ascaroside cocktail along with DA hormone [18] (Figures S1B and S1C). Our second approach also uses the ascaroside cocktail, but to eliminate the need for DA hormone, dauer-commitment-defective *daf-12(rh61)* mutant worms are employed. In the third approach, to genetically induce L2d, we combined *daf-12(rh61)* with a temperature-sensitive *daf-7* mutant that mimics the L2d-inducing pheromone conditions or with a temperature-sensitive *daf-2* mutant that mimics the L2d-inducing starvation conditions.

L2d-Inducing Ascarosides Reduce the Reliance on the *let-7* Family MicroRNAs for Proper L2-to-L3 Cell-Fate Transition

Wild-type larvae robustly execute L2-stage cell fates and transition to L3-stage cell fates (thus, # of seam cell = 16 in young adult worms) regardless of developmental trajectory (Figure 2, rows 1–3). *mir-48/84/241(0)* triply-mutant larvae reiterate L2-stage cell fates at later stages due to prolonged HBL-1 expression, resulting in extra (>16) seam cells in young adult animals (Figure 2, row 4). We found that when *mir-48/84/241(0)* mutant larvae developed through L2d—induced by a combination of the ascaroside cocktail and the DA hormone—the extra seam cell phenotype was substantially (albeit partially) suppressed (Figure 2, row 4 versus 6). To compare the strength of this L2d suppression with the previously described post-dauer suppression of the *let-7* family phenotypes [13], we used the ascaroside cocktail but this time without the DA hormone. Under these conditions, *mir-48/84/241(0)* larvae arrested as dauers; and as described previously [13], this resulted in complete suppression of the extra seam cell phenotype in post-dauer adults (Figure 2, row 4 versus 5). Therefore, the L2d suppression is weaker than the post-dauer suppression (Figure 2, row 6 versus 5), and unlike dauer arrest, L2d-inducing ascarosides do not completely eliminate the need for *let-7* family microRNAs for proper L2-to-L3 cell-fate transition. Nonetheless, the partial suppression of the extra seam cell phenotype of *let-7* family microRNAs suggests that the L2d-inducing ascarosides rewire the genetic regulatory pathway controlling temporal cell-fate progression in a way to

reduce the reliance on the *let-7* family microRNAs for proper L2-to-L3 cell-fate transition.

L2d-Inducing Ascarosides or L2d-Inducing Mutations of *daf-7* and *daf-2* Suppress Heterochronic Phenotypes Caused by Insufficient Expression of *let-7* Family MicroRNAs in *daf-12(rh61)* Mutants

The *daf-12(rh61)* mutation combines three important properties, which makes this mutation uniquely useful for studying the effects of L2d-inducing conditions on the regulation of temporal cell fates. These properties are as follows: (1) *daf-12(rh61)* animals reiterate expression of L2 cell fates owing to reduced (insufficient) *let-7* family levels; (2) *daf-12(rh61)* larvae are unable to execute dauer larvae commitment or arrest [19], enabling the use of dauer-promoting conditions to obtain populations of *daf-12(rh61)* animals undergoing an L2d-direct-to-L3 continuous development trajectory; and (3) *daf-12(rh61)* animals are insensitive to the DA hormone (due to lack of the DAF-12 ligand binding domain) [18, 19], and so the levels of *let-7* family microRNAs are expected to be unresponsive to experimentally administered ascarosides, which are understood to regulate wild-type DAF-12 activity by affecting the level of DA [10].

We observed that the presence of exogenous ascaroside cocktail during larval development almost completely suppressed the extra seam cell phenotype of *daf-12(rh61)* mutants (Figure 2, row 7 versus 8). To test the possibility that an unexpected elevation in the *let-7* family levels could be responsible for the suppression of the heterochronic phenotypes of *daf-12(rh61)* animals in the presence of the ascaroside cocktail, we quantified the levels of *let-7* family microRNAs in the absence and presence of the ascarosides (Figure S2). No elevation in the levels of these microRNAs in response to the ascaroside cocktail was evident (Figure S2). Therefore, the suppression of the heterochronic phenotypes of *daf-12(rh61)* mutants in the presence of the ascaroside cocktail is unlikely to result from restoration of normal levels of *mir-48/84/241* or an elevation of the other members of the *let-7* family microRNAs (Figure S2).

Similar to the ascaroside cocktail, conditional dauer-constitutive mutants of *daf-7* (mimicking high ascarosides) or *daf-2* (mimicking starvation) that allow continuous (L2d-to-L3 without dauer arrest) development at permissive temperatures [20] almost completely suppressed the extra seam cell phenotype of *daf-12(rh61)* mutants (Figure 2, row 7 versus 9 or 10). These results indicate that genetically induced L2d, whether by activation of the ascaroside response pathway (*daf-7(lf)*) or by activating the starvation response pathway (*daf-2(lf)*), results in an L2d-associated rewiring of the regulatory networks controlling temporal cell-fate progression.

Ascarosides Suppress the Heterochronic Phenotypes of *daf-12(rh61)* via *srg-36/37*-Encoded GPCR Signaling Upstream of DAF-7/TGF- β -DAF-3 Signaling

Each of the individual ascarosides in the cocktail (*ascr#2*, 3, and 5) has been shown previously to be alone sufficient to induce dauer formation, although with reduced potency compared to the combined cocktail [17, 21]. Consistent with their individual capacities to induce L2d and dauer formation, we observed that each ascaroside *ascr#2*, *ascr#3*, and *ascr#5* alone could suppress the extra seam cell phenotype of *daf-12(rh61)* mutants

(Figure S3A). In the case of *ascr#2* or *ascr#3* alone, the suppression was partial, while for *ascr#5* alone, the suppression was similar to that of the full cocktail (Figure S3A, rows 6 to 10). *ascr#5* was the most potent of the three ascarosides in terms of both percent dauer formation of wild-type larvae (Figure S3B) and suppression of the extra seam cell phenotype of *daf-12(rh61)* (Figure S3A, row 10 versus 8 and 9).

It has been shown previously that induction of dauer formation by ascarosides involves sensing of environmental ascaroside levels by specific G-protein coupled receptors (GPCRs) expressed in chemosensory neurons, wherein they repress DAF-7/TGF- β signals [22–25]. To test whether these GPCRs were also required for the suppression of the heterochronic phenotypes of *daf-12(rh61)* mutants, we employed mutations of *srg-36* and *srg-37*, which encode GPCRs that are expressed in the ASI neurons and that are redundantly required for perceiving *ascr#5* signal in the context of dauer induction [24]. We observed that for *srg-36(0) srg-37(0); daf-12(rh61)* compound mutants, ascaroside (in this case *ascr#5*) failed to suppress the extra seam cell phenotype *daf-12(rh61)* (Figure 3A, compare row 1 versus 2 with row 3 versus 4). Moreover, we found that the TGF- β signaling effector *daf-3*, which is thought to function downstream of SRG-36/37, is required for the suppression of *daf-12(rh61)* by ascaroside (Figure 3B). These results indicate that the same GPCRs that mediate dauer formation in response to ascaroside are also required for mediating the effects of ascaroside on temporal cell fates and support a common pathway for suppression of *daf-12(rh61)* by ascaroside and dauer induction, involving activation of SRG-36/37 GPCRs and the potential downstream TGF- β effector DAF-3.

DAF-7/TGF- β and DAF-2/Insulin Signaling Pathways Act in Parallel to Mediate the Suppression of the Heterochronic Phenotypes of *daf-12(rh61)*

As shown above, genetic activation of dauer-inductive signaling by *daf-7(lf)* or *daf-2(lf)* mutations is sufficient for suppression of *daf-12(rh61)* (Figure 2). In the context of dauer formation, DAF-7/TGF- β primarily mediates ascaroside signaling, and DAF-2/Insulin primarily mediates assessment of nutritional status [10, 22, 26]. To determine if the known downstream effectors of DAF-7/TGF- β and DAF-2/Insulin signaling that mediate dauer formation are also required for mediating the L2d rewiring caused by *daf-7(lf)* or *daf-2(lf)* [27, 28], we generated compound mutants carrying *daf-12(rh61)* in combination with mutations that impair these effectors of the TGF- β or insulin signaling pathways and determined the number of seam cells in young adults. We found that the downstream effector of the TGF- β signaling pathway, *daf-3*, and the downstream effector of the insulin signaling pathway, *daf-16*, were required for the suppression mediated by the *daf-7(lf)* mutation and the *daf-2(lf)* mutation, respectively (Figures 3C and 3D). These results are consistent with the finding that *daf-3* was also required for the ascaroside-mediated suppression of *daf-12(rh61)* (Figure 3B).

To determine whether the TGF- β and insulin signaling pathways act in parallel to modulate temporal cell fates, we tested for crosstalk between these pathways in the context of suppression of *daf-12(rh61)* phenotypes. Specifically, we determined whether *daf-16(lf)* could alter the suppression of *daf-12(rh61)* phenotypes by *daf-7(lf)* and conversely, whether *daf-3(lf)* could

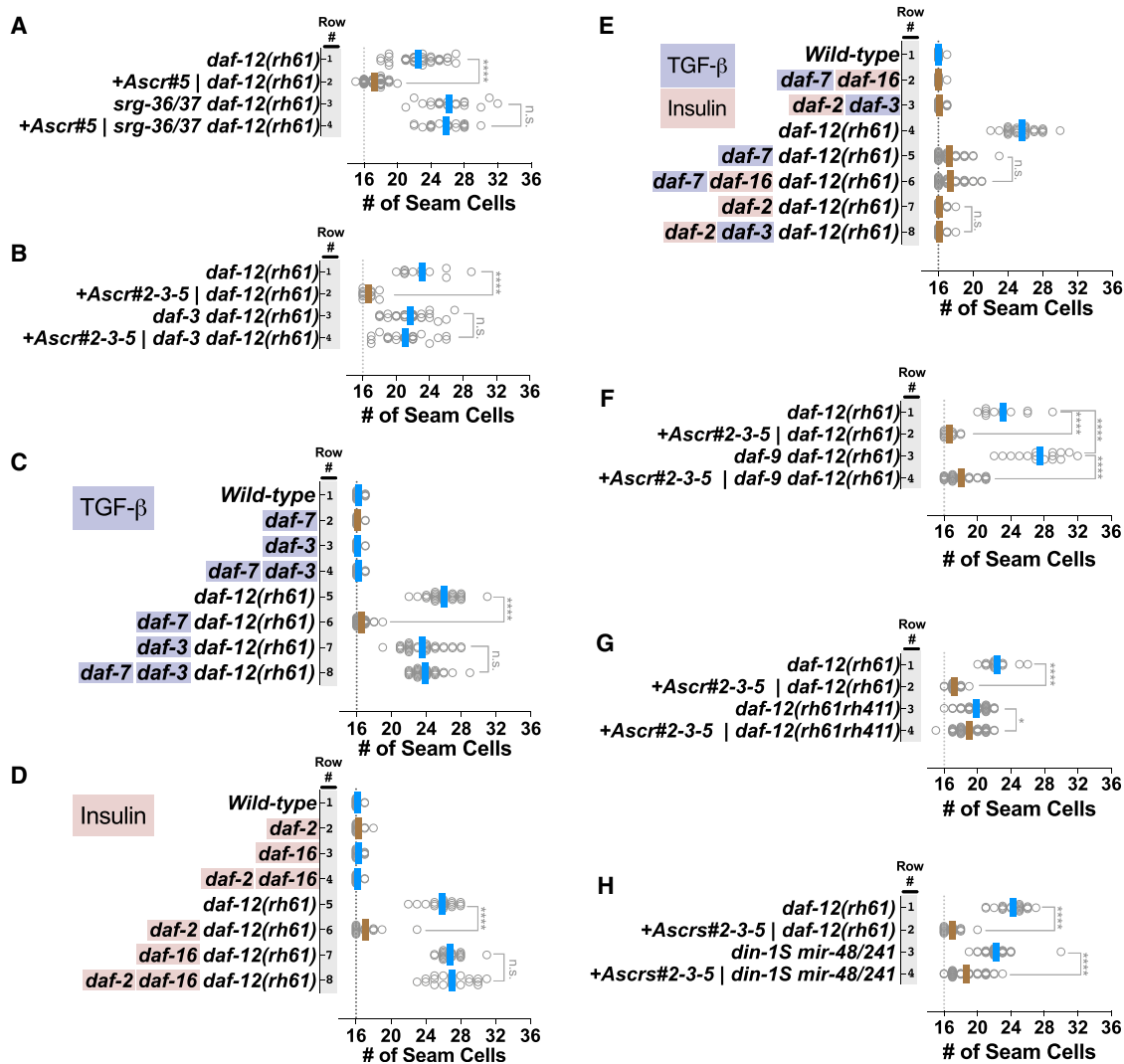


Figure 3. DAF-7/TGF- β and DAF-2/Insulin Signaling Pathways Act in Parallel to Modulate a Ligand-Independent Activity of DAF-12 That Is Responsible for Correcting Heterochronic Phenotypes Caused by Insufficient Expression of *let-7* Family MicroRNAs

Number of seam cells in young adult animals of various mutants cultured on ascaroside or control plates (A, B and F, G), or on standard NGM plates (C–E): each dot in the plots shows the number of seam cells of a single young adult animal, and solid lines indicate the average seam cell number of the animals scored for each condition (blue lines, rapid trajectory; brown lines, L2d trajectory).

(A) Ascarosides suppress *daf-12(rh61)* via *srg-36/37*-encoded GPCR signaling upstream of DAF-7/TGF- β -DAF-3 signaling.

(B) *daf-3* activity is required for suppression of *daf-12(rh61)* by ascarosides.

(C–E) DAF-7/TGF- β and DAF-2/Insulin signaling pathway act in parallel to mediate the suppression of *daf-12(rh61)*.

(F and G) Ligand-independent activity of *daf-12* is required for the ascaroside-mediated L2d rewiring of the pathways regulating temporal cell fates.

(H) The DAF-12 corepressor DIN-1S is not required for the ascaroside-mediated suppression of heterochronic phenotypes caused by insufficient expression of *let-7* family microRNAs. Suppression of extra seam cell phenotype of *daf-12(rh61)* is shown as a measure of the strength of the ascaroside conditions tested for *din-1S(lf)*; *mir-48/241(lf)* animals. The Student's *t* test is used to calculate statistical significance (*p*): n.s. (not significant) $p > 0.05$, * $p < 0.05$, ** $p < 0.01$, *** $p < 0.001$, **** $p < 0.0001$.

See also Figure S3 and Table S1.

alter the suppression of *daf-12(rh61)* phenotypes by *daf-2(lf)*. We found that *daf-16* was not required for *daf-7*-mediated suppression (Figure 3E, rows 5 and 6), and *daf-3* was not required for *daf-2*-mediated suppression (Figure 3E, rows 7 and 8), indicating that, similar to their regulation of dauer diapause, the TGF- β and insulin signaling pathways act in parallel in the context of the L2d rewiring of the genetic regulatory pathways controlling larval cell-fate progression.

Ligand-Independent Activity of *daf-12* Is Required for the Ascaroside-Mediated L2d Rewiring of the Pathways Regulating Temporal Cell Fates

Ascaroside (TGF- β) signaling and nutritional status (insulin) signaling converge to induce dauer larva arrest by downregulating DA production and hence reducing the levels of liganded DAF-12 [10]. Since we find that dauer-inducing conditions (ascarosides; loss of *daf-7* or *daf-2*) can suppress the heterochronic

phenotypes of the DA-insensitive *daf-12(rh61)* mutant, it would appear that the TGF- β and insulin signaling pathways may regulate cell-fate transitions by repressing a hypothetical DAF-12-independent function of DA. If that were the case, inhibiting or preventing DA production would mimic the effect of ascarosides and suppress the extra seam cell phenotype of *daf-12(rh61)*. To test this possibility, we employed genetic ablation of DA production. *daf-9* encodes a CYP450 that is responsible for DA production [18]. Accordingly, *daf-9(lf)* mutants are dauer-constitutive due to lack of DA [18]. To test if ascarosides act by inhibiting DA production during L2d rewiring, we generated double mutants containing *daf-9(lf)* and *daf-12(rh61)*. We observed that these double mutants lacking *daf-9* in the *daf-12(rh61)* background had an even stronger extra seam cell fate phenotype than *daf-12(rh61)* mutants (Figure 3F, row 1 versus 3) and that this phenotype was suppressed in the presence of ascarosides (Figure 3F, row 3 versus 4). These results indicate that the ascaroside-induced L2d rewiring does not involve inhibition of DA biosynthesis, and nor does rewiring require DA production or *daf-9* activity. The enhancement of the extra seam cell phenotype of *daf-12(rh61)* phenotype in the *daf-12(rh61); daf-9(lf)* double mutant could reflect DAF-12-independent functions of DA or DA-independent functions of DAF-9.

The finding that ascaroside-mediated L2d rewiring did not involve the DA hormone raised the question as to whether the DA receptor, DAF-12, is required for the L2d rewiring. To determine whether *daf-12* is required for ascaroside-induced suppression of retarded seam cell phenotypes, we tested whether ascarosides could suppress the phenotypes of *daf-12(rh61rh411)*, a *daf-12* null allele [19]. *daf-12(rh61rh411)* animals display a milder extra seam cell phenotype than do *daf-12(rh61)* [19] animals, presumably because of a milder reduction of *let-7* family microRNAs compared to *daf-12(rh61)* [16]. We observed that the ascaroside conditions that resulted in a very potent suppression of the extra seam cell phenotype of *daf-12(rh61)* animals resulted in only a very modest (albeit statistically significant) suppression of the *daf-12(rh61rh411)* phenotype (Figure 3G, compare changes in the average number of seam cells in row 1 versus 2 with 3 versus 4). This result suggests that ascaroside-induced L2d rewiring of the pathways regulating temporal cell fates largely requires *daf-12* function and therefore represents a novel ligand-independent regulation of *daf-12* by TGF- β and insulin signaling.

The DAF-12 Corepressor DIN-1S Is Not Required for the Ascaroside-Mediated Suppression of Heterochronic Phenotypes Caused by Insufficient Expression of *let-7* Family MicroRNAs

When DA is absent, DAF-12 interact with DIN-1S, and together they form a repressive complex that is necessary for dauer formation [18, 29]. *din-1S(lf)* suppresses heterochronic phenotypes of *daf-12(rh61)* [29], likely by relieving repression of *let-7* family microRNA transcription. Therefore, it was possible that the ascaroside-mediated suppression of the heterochronic phenotypes of *daf-12(rh61)* could reflect ascaroside-induced downregulation of *din-1S* activity. To assess the potential involvement of *din-1S* in ascaroside-mediated suppression of the phenotypes caused by reduced *let-7* family microRNAs, we tested for ascaroside suppression of a compound mutant lacking *mir-48/*

241 and *din-1S* (Figure 3H). We observed that *din-1(lf)* did not prevent ascaroside suppression of the *mir-48/241* extra seam cell phenotypes (Figure 3H, row 3 versus 4), indicating that DIN-1S is not required for ascaroside-mediated L2d rewiring.

Heterochronic Genes Previously Associated with the Altered HBL-1 Downregulation Program in Post-Dauer Animals Are Required for the L2d Suppression of Heterochronic Phenotypes Caused by Insufficient Expression of *let-7* Family MicroRNAs

In animals that arrested as dauer larvae and then later resumed development through post-dauer larval stages, the genetic programming of temporal cell fates differed substantially from that in animals that developed continuously [13]. In particular, proper cell-fate progression through dauer larvae arrest and post-dauer development depends on an altered HBL-1 downregulation program. These differences in HBL-1 downregulation include (1) reallocation of roles for *lin-4* microRNA and *let-7* family microRNAs and (2) alterations in the relative impacts of LIN-46 and the microRNA modulatory factor NHL-2 [13]. For example, animals deficient for *lin-4* exhibited stronger retarded developmental timing phenotypes when traversing developmental arrest followed by post-dauer development compared to animals of the same genotype that developed rapidly and continuously. Similarly, animals carrying loss-of-function mutations of *nhl-2* or *lin-46* exhibited enhanced retarded phenotypes after post-dauer development. *nhl-2* encodes an RNA binding protein that functions as a microRNA positive modulator [30], and *lin-46* encodes a protein that acts downstream of the LIN-28 RNA binding protein [31]. These results suggested that the rewiring of developmental cell-fate progression in dauer-traversing larvae involves alterations in the post-transcriptional regulation of HBL-1 expression.

To confirm that L2d-inducing conditions resulted in HBL-1 downregulation, we tagged *hbl-1* at its endogenous locus with mScarlet-I using CRISPR/Cas9 genome editing (see STAR Methods) and monitored the level of HBL-1::mScarlet-I expression in developing larvae. We compared HBL-1 expression in L2- and L3-stage *daf-12(rh61)* larvae to that in L2d- and L3-stage larvae of the suppressed *daf-7(lf); daf-12(rh61)* double mutants (Figure 4A). At the L2/L2d stage, HBL1 expression in *daf-12(rh61)* and *daf-7(lf); daf-12(rh61)* were comparable (Figure 4A, L2/L2d). At the L3 stage, however, whereas HBL-1 was overexpressed in both seam and hyp7 cells of *daf-12(rh61)* animals, HBL-1 was absent in the seam cells of *daf-7(lf); daf-12(rh61)* animals (Figure 4A, L3). This downregulation of HBL-1 expression in seam cells of *daf-7(lf); daf-12(rh61)* mutants is consistent with the suppression of extra seam cell phenotypes of *daf-12(rh61)* by *daf-7(lf)*.

To test whether the previously described genetic requirements for *lin-46*, *lin-4*, and *nhl-2* to downregulate HBL-1 in the dauer or post-dauer context [13] also apply during L2d development, we examined the phenotypes of the relevant mutant strains during development through ascaroside-induced L2d, but in this case, without dauer commitment or arrest. We observed that ascarosides failed to suppress the retarded phenotypes of animals that were lacking *lin-46* or *lin-4* in combination with *mir-84(lf)* (to provide a sensitized background, blunting the expression of *let-7* family microRNAs) or were lacking *nhl-2* in the *daf-12(rh61)*

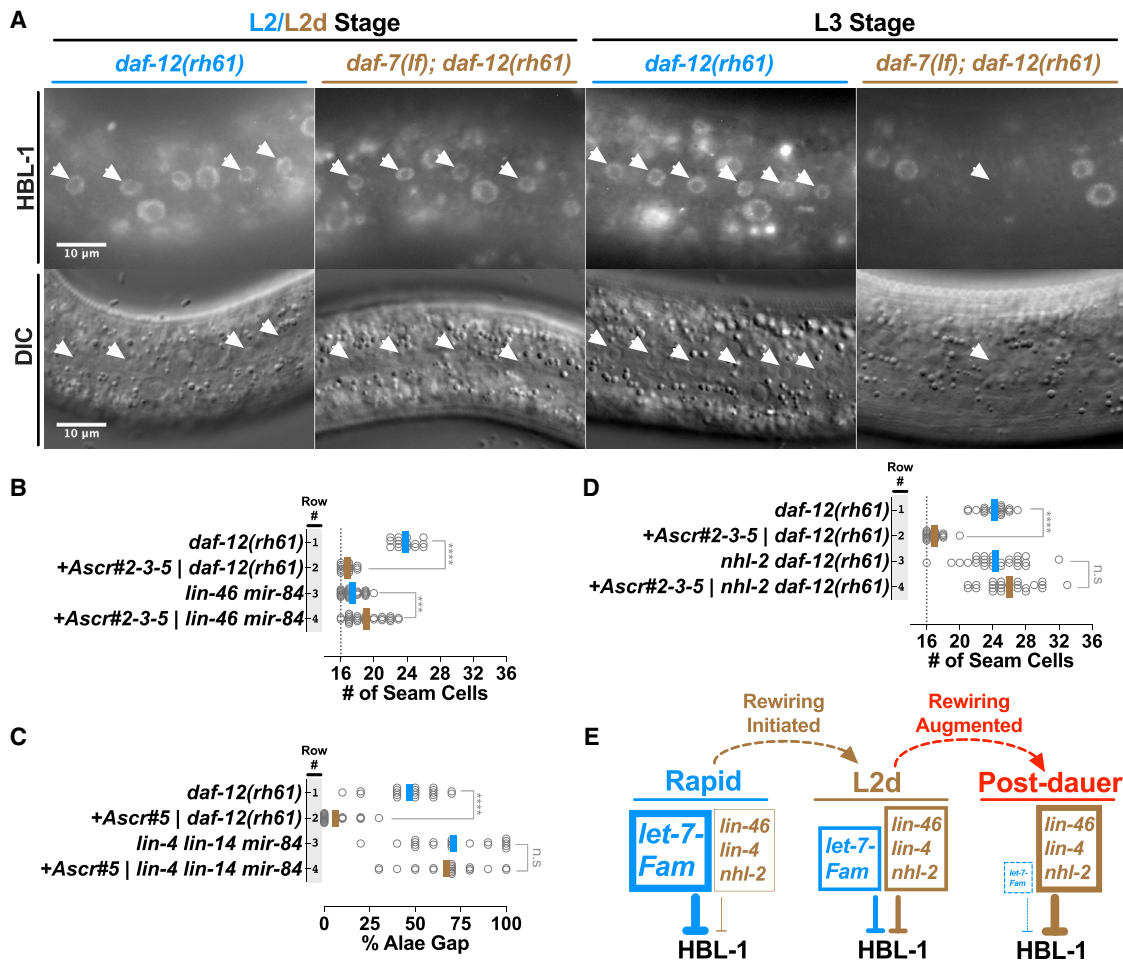


Figure 4. Heterochronic Genes Associated with the Altered HBL-1 Downregulation Program in Post-Ddauer Animals Are Required for the L2d Suppression of Heterochronic Phenotypes Caused by Insufficient Expression of *let-7* Family MicroRNAs

(A) Upper row: fluorescent images showing HBL-1 expression in L2/L2d and L3 stage hypodermal seam (white arrowheads) and hyp7 (all other) nuclei in *daf-12(rh61)* and *daf-7(lf); daf-12(rh61)* animals. Lower row: corresponding DIC images of the hypodermis. It should be noted that, consistent with the variability in the extra seam cell phenotype of *daf-12(rh61)* animals, HBL-1 expression at the L3-stage *daf-12(rh61)* animals displays variability across seam cells of individual worms. For example, HBL-1 expression may be present and absent in two neighboring seam cells, which presumably express L2 and L3 cell fates, respectively.

(B) Ascaroside conditions that suppress the extra seam cell phenotype of *daf-12(rh61)* enhance the extra seam cell phenotype of larvae lacking *lin-46* and *mir-84*. (C) Ascaroside conditions that suppress the gapped alae (a consequence of retarded seam cell development that is manifested in young adults) phenotype do not suppress the gapped alae phenotype of *lin-4; lin-14; mir-84* animals.

(D) *nhl-2* activity is required for ascaroside-mediated suppression of *daf-12(rh61)*.

(E) A model for the L2d rewiring and its potential augmentation during dauer arrest. Under L2d-inducing conditions, *let-7* family microRNAs are downregulated and also become less important. The reduction in the *let-7* family level and importance is coupled to enhanced roles for the heterochronic genes previously associated with the altered HBL-1 downregulation program in post-ddauer animals, involving *lin-46*, *lin-4*, and *nhl-2*. This shift in the reliance on the *let-7* family microRNAs to the reliance on the alternative program for proper HBL-1 downregulation (hence, for proper L2-to-L3 cell-fate progression) constitutes the L2d rewiring. In post-ddauer animals, consistent with an augmentation of the L2d rewiring program, the reliance on the altered HBL-1 downregulation program further increases while the *let-7* family microRNAs become dispensable for proper HBL-1 downregulation. It should be noted that we do not know the mechanisms (e.g., elevated levels versus enhanced activities) of increased roles for *lin-46*, *nhl-2*, or *lin-4* during L2d or post-ddauer development. The Student's *t* test is used to calculate statistical significance (p): n.s. (not significant) $p > 0.05$, * $p < 0.05$, ** $p < 0.01$, *** $p < 0.001$, **** $p < 0.0001$.

See also Table S1.

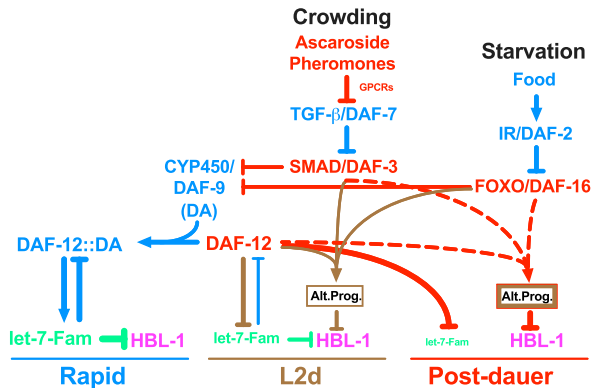
background. (Figures 4B–4D). Moreover, for doubly-mutant animals carrying both *mir-84(lf)* and *lin-46(lf)* mutations, ascaroside-induced L2d enhanced the retarded phenotypes (Figure 4B), similar to the enhancement reported for *mir-84(lf); lin-46(lf)* animals that developed through dauer arrest and post-ddauer development [13]. Similarly, ascarosides failed to suppress the gapped alae phenotype of animals lacking *lin-4* and *mir-84*

(Figure 4C), consistent with the previous finding that this phenotype of *lin-4(lf); mir-84(lf)* animals was enhanced for post-ddauer animals [13]. Lastly, ascarosides failed to suppress the extra seam cell phenotypes of *nhl-2; daf-12(rh61)* animals (Figure 4D), indicating that *nhl-2* is required for ascaroside-mediated suppression of *daf-12(rh61)*, analogous to its role in post-ddauer enhancement of the retarded phenotypes of *let-7* family

A Alternative Trajectories



B L2d Rewiring and Dauer Augmentation



C Kinetics of Gene Activities

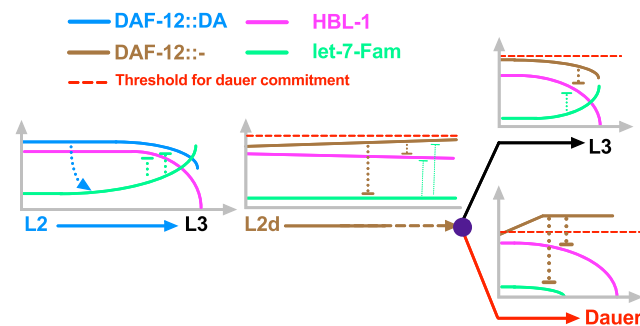


Figure 5. Coordinate Regulation of Developmental Progression and Cell-Fate Transitions in *C. elegans* Larvae

(A) Alternative trajectories. The L2-to-L3 transition is rapid and deterministic (once committed to the L2 stage, the larvae do not have the dauer option), whereas the L2d-to-L3 transition is slower and bipotential. In both cases, HBL-1 is present throughout the L2/L2d stage, but it is downregulated by the beginning of the L3 stage (Figure S4).

(B) Pheromone and endocrine signals engage DAF-12 to initiate and regulate the rewiring of the HBL-1 downregulation. In response to crowding and starvation, TGF- β and insulin signaling pathways, respectively, modulate the ligand-dependent DAF-12 activity to repress the transcription of *let-7* family microRNAs and, at the same time, cooperate with DAF-12 in a ligand-independent manner to activate the alternative HBL-1 downregulation program (Alt. Prog.). The alternative program of L2d and dauer-interrupted trajectories are similar, but the alternative program of dauer-interrupted trajectory is stronger either due to an enhancement of the alternative program of L2d (depicted by thicker brown border) and/or due to employment of additional factors (depicted as bold red line) after the L2d larvae commit to dauer formation.

(C) DAF-12 ensures properly delayed but robust HBL-1 downregulation during L2d-to-L3 transition by coordinating the repression of *let-7* family microRNAs with the activation of the alternative HBL-1 downregulation program. During rapid, L2 development, DAF-12 activates the transcription of *let-7* family microRNAs, which in turn negatively regulate DAF-12, eliminating the dauer option. During slow, bipotential, L2d development, DAF-12 represses *let-7* family microRNAs, which otherwise would have prevented the accumulation of DAF-12. If the unliganded DAF-12 reaches a threshold, larvae commit to dauer formation; if not, larvae commit to continuous development. While mediating this decision, which necessitates the repression of *let-7* family microRNAs (for

maintaining the dauer option) and delaying the downregulation of HBL-1 (for postponing L3 cell fates), DAF-12 cooperates with DAF-3 or DAF-16 to activate the alternative HBL-1 downregulation program (Alt. Prog.) to ensure robust HBL-1 downregulation during the L2d-to-L3 transition. See also Figure S4.

DISCUSSION

Environmental and physiological stress signals can challenge the progression of *C. elegans* larval development, causing the larva to choose one of three distinct alternative developmental trajectories: (1) a rapid and continuous trajectory without the option for dauer arrest; (2) continuous development through an extended, bipotent L2d trajectory, wherein the option for dauer arrest is enabled, but not necessarily selected; and (3) development through the L2d trajectory followed by dauer larva arrest (Figure 5A). Regardless of which trajectory is chosen by the larva, the same sequence of stage-specific cell fates is robustly expressed (Figure 1A and Figure 2, rows 1–3). The findings reported here illuminate how genetic regulatory networks that specify larval cell-fate progression can accommodate these alternative life histories and the physiological and environmental stresses that induce them.

Central to the coordination of temporal cell fates and life history choices in *C. elegans* is the nuclear hormone receptor transcription factor DAF-12 [19] and its ligand, dafachronic acid (DA) [18]. DAF-12 in the unliganded form is essential for the dauer larva trajectory, while ligand-bound DAF-12 inhibits the L2-to-L3 cell-fate transitions by regulating the expression of *let-7* family microRNAs, which are required to downregulate HBL-1 and thereby specify the proper timing of expression of L3 cell fates [6, 16, 18, 32].

The *let-7* family microRNAs also regulate the abundance of DAF-12 via a feedback loop that has been proposed to help ensure robust coordination of cell fates with dauer arrest [16]. Under favorable conditions, when DA is abundant, DA-bound DAF-12 promotes continuous development and also activates accumulation of *let-7* family microRNAs during the L2 stage, which in turn attenuate the accumulation of DAF-12 (thereby eliminating the dauer option) and also downregulate HBL-1 to enable rapid progression from L2 to L3 cell fates. Conversely, under unfavorable conditions, DA production is low, and unliganded DAF-12 promotes the L2d and dauer program and represses the expression of *let-7* family microRNAs. In turn, the low level of *let-7* family microRNAs allows the accumulation of DAF-12 during L2d, maintaining the dauer option [16].

maintaining the dauer option) and delaying the downregulation of HBL-1 (for postponing L3 cell fates), DAF-12 cooperates with DAF-3 or DAF-16 to activate the alternative HBL-1 downregulation program (Alt. Prog.) to ensure robust HBL-1 downregulation during the L2d-to-L3 transition. See also Figure S4.

It was not previously clear how HBL-1 might be downregulated during L2d considering the repressed state of the *let-7* family microRNAs. We propose that the L2d program instigated by unliganded DAF-12 includes, in addition to the repression of *let-7* family microRNAs, the activation of an alternative mechanism of HBL-1 downregulation (Figure 5B), which is responsible for the suppression of *daf-12(rh61)* by ascarosides (Figure 2, row 8) and by L2d-inducing mutants of *daf-7* and *daf-2* (Figure 2, rows 9 and 10). The L2d suppression of *daf-12(rh61)* phenotypes led us to propose that during wild-type L2d, when DA is low, DAF-12 is unliganded, and its activity is hence not unlike that of the ligand-binding defective mutant DAF-12(RH61). In this model, we propose that *daf-12(rh61)* animals constitutively run an “L2d-like program” for regulating temporal cell fates, which is discordant with rapid continuous development but compatible with (and hence phenotypically suppressed by) the environmental and endocrine signals that induce the L2d trajectory.

Our conclusion that a DA-independent function of DAF-12 is required for the modulation of temporal cell fates during L2d is derived from our finding that the mild retarded phenotype of the *daf-12* null allele, *daf-12(rh61rh441)*, was not suppressed by ascarosides, in contrast to the stronger retarded phenotype of *daf-12(rh61)*, which is efficiently suppressed (Figure 3G). Consistent with our results showing the requirement for *daf-12* for L2d rewiring, a *daf-2(lf)* mutant was reported to not suppress (indeed, to enhance) the extra seam cell phenotypes of *daf-12(lf)* [33].

We find that the DA-independent function of DAF-12 that modulates temporal cell fates during the L2d can be activated by either of the two upstream transcription factors, DAF-3, which mediates responses to TGF- β signaling from ascaroside-sensing neurons, and DAF-16, which mediates DAF-2 (IGF) signaling. We hypothesize that DAF-12 cooperates with DAF-3 or DAF-16 in a DA-independent manner to activate and modulate the alternative HBL-1 downregulation program (Figure 5B). Although the immediate action of DAF-12, together with DAF-3 or DAF-16, would likely be transcriptional, ultimately, the alternative pathway for HBL-1 downregulation appears to be post-transcriptional, as we found that suppression of *daf-12(rh61)* or *mir-84(lf)* by L2d involves contributions from *lin-4* and *let-7* family microRNAs in addition to the miRISC cofactor NHL-2 [30] and also LIN-46, which is thought to function post-transcriptionally [31]. Interestingly, the alternative HBL-1 downregulation program appears to be activated in seam cells but not in hyp7 cells (Figure 4A), which is distinctly different from the *let-7* family regulation of HBL-1 occurring both in the seam and hyp7 cells.

Prior to this study, it was not clear whether the inhibition of dauer larva formation by exogenously-supplied DA reflects prevention of L2d in addition to a block of dauer-commitment. We observed that exogenous DA hormone at levels sufficient to prevent ascaroside-induced dauer formation does not prevent the extension of second-larval-stage development characteristic of L2d. Also, we observed that *daf-12(rh61)* animals, which are DA-insensitive and dauer-commitment defective, nevertheless can readily undergo L2d. These observations suggest that L2d is initiated independently of DAF-12-DA activity and are consistent with our model that a DA-independent function of DAF-12, together with activated DAF-3 or DAF-16, promote expression of the L2d program.

The studies described here involve animals that traverse the bi-potential L2d stage but elect the option of resuming L3 development instead of dauer larva arrest. Previous studies showed that for animals that enter dauer diapause arrest and later are induced to emerge from dauer arrest and complete post-dauer L3 and L4 development, a similar change in the HBL-1 downregulation program is evident [13]. Here we show that the genetic circuitry controlling cell-fate progression via HBL-1 in larvae undergoing L2d development is similar to the circuitry previously identified for animals that arrest as dauer larvae [13]. In particular, we find that *lin-4* and NHL-2 have similarly prominent roles in both the L2d-only and the post-dauer trajectories. Moreover, for both the L2d-to-L3 trajectory and the L2d-to-dauer-to-post-dauer trajectory, an enhanced role for *lin-46* is evident, compared to the rapid continuous-development trajectory. Our finding of an increased importance of LIN-46 during the L2d is consistent with a previous report that a *daf-2(lf)* mutation could enhance the retarded phenotype of *sea-2(lf)* [33], whose phenotype presumably reflects elevated *lin-28* activity and hence reduced *lin-46* activity.

These results—that the rewiring of HBL-1 downregulation for the L2d-only trajectory is largely similar to that for dauer-postdauer trajectory—are consistent with the fact that dauer larvae arrest is always preceded by L2d. Therefore, the rewiring associated with traversing post-dauer likely is initiated during L2d. The observation that suppression of the retarded phenotypes of certain mutants is more potent for the L2d-dauer-postdauer trajectory compared to the L2d-only trajectory (Figure 2, row 5 versus 6) suggests that rewiring may be partially implemented during L2d and more fully engaged in association with dauer commitment (Figure 5B).

Our observations of the kinetics of HBL-1 downregulation during the L2 and L2d stages (Figure S4) suggest that HBL-1 levels are maintained at relatively high levels for much of the L2 or L2d stage and downregulated near the end of the stage (Figure 5C and Figure S4). This suggests that downregulation of HBL-1, and hence commitment to L3 cell-fate specification, may be gated by some event(s) coupled to the completion of the L2 or L2d stage. This would be consistent with a model wherein most of the L2d is occupied by rewiring of pathways upstream of HBL-1, followed by implementation of HBL-1 downregulation at the end of the L2d, in association with commitment to the L3 cell fate.

In summary, we show that environmental and endocrine stress signals that regulate developmental progression and alternative developmental trajectories rewire the genetic regulatory network controlling temporal cell-fate transitions during larval development of *C. elegans*. Our findings provide insight into how the regulation of temporal cell-fate transitions can be adapted to accommodate stressful conditions that challenge developmental progression. Coordinate regulation of developmental progression and temporal cell fates seems to confer elasticity to *C. elegans* development, wherein the proper developmental schedule of cell-fate transitions is unaffected by variations in developmental rate or developmental trajectory.

C. elegans larvae possess other life history options in addition to the delayed developmental progression associated with the L2d-dauer trajectory. For example, appropriate pheromone signals and nutritional status can result in an acceleration of *C. elegans* development [34–36]. Moreover, larvae can

temporarily suspend developmental progression at specific checkpoints in the late L2, L3, or L4 stages in response to acute starvation [37]. We hypothesize that these signals that either accelerate development or result in programmed developmental arrest would also be associated with appropriate rewirings of the genetic regulatory pathways regulating temporal cell-fate progression so that cell-fate transitions are appropriately synchronized with the dynamics of larval stage progression. Lastly, rewiring mechanisms induced by environmental signals, such as that described here, might also be adapted for the evolution of morphological plasticity or polyphenism observed in certain nematodes [38, 39] and other animals [40].

STAR★METHODS

Detailed methods are provided in the online version of this paper and include the following:

- **KEY RESOURCES TABLE**
- **CONTACT FOR REAGENT AND RESOURCE SHARING**
- **EXPERIMENTAL MODEL AND SUBJECT DETAILS**
 - *C. elegans* culture conditions
- **METHOD DETAILS**
 - Dauer and L2d-inducing plates
 - Analysis of extra seam cell phenotypes
 - TaqMan assays for microRNA quantification
 - Tagging of *hbl-1* at its endogenous locus
 - Plasmid DNA purification and microinjection of worms
 - Cloning of sgRNA plasmids
 - Cloning of pOI191 HR template plasmid
 - Microscopy imaging of *C. elegans* larva
- **QUANTIFICATION AND STATISTICAL ANALYSIS**

SUPPLEMENTAL INFORMATION

Supplemental Information can be found online at <https://doi.org/10.1016/j.cub.2019.04.034>.

ACKNOWLEDGMENTS

We thank the Schroeder (Cornell) and Srinivasan (WPI) laboratories for providing ascariosides and the Bargmann (Rockefeller) laboratory for sharing the *srg-36/37* mutant strains. We thank the members of the Mello (UMass Medical) and Ambros laboratories for helpful discussions and the members of the Ambros laboratory and Micah Belew for critical reading of the manuscript. This research was supported by funding from NIH grants R01GM088365 and R01GM034028 (V.A.). Some *C. elegans* strains were provided by the *Caenorhabditis* Genetics Center (University of Minnesota), which is funded by NIH Office of Research Infrastructure Programs (P40 OD010440).

AUTHOR CONTRIBUTIONS

O.I. conducted the experiments, and O.I. and V.A. designed the experiments, interpreted the results, and wrote the paper.

DECLARATION OF INTERESTS

The authors declare no competing interests.

Received: February 11, 2019

Revised: April 3, 2019

Accepted: April 11, 2019

Published: May 16, 2019

REFERENCES

1. Sulston, J.E., and Horvitz, H.R. (1977). Post-embryonic cell lineages of the nematode, *Caenorhabditis elegans*. *Dev. Biol.* *56*, 110–156.
2. Ambros, V., and Horvitz, H.R. (1984). Heterochronic mutants of the nematode *Caenorhabditis elegans*. *Science* *226*, 409–416.
3. Ambros, V. (2011). MicroRNAs and developmental timing. *Curr. Opin. Genet. Dev.* *21*, 511–517.
4. Lin, S.Y., Johnson, S.M., Abraham, M., Vella, M.C., Pasquinelli, A., Gamberi, C., Gottlieb, E., and Slack, F.J. (2003). The *C. elegans* hunchback homolog, *hbl-1*, controls temporal patterning and is a probable microRNA target. *Dev. Cell* *4*, 639–650.
5. Abraham, J.E., Daul, A.L., Li, M., Volk, M.L., Tennesen, J.M., Miller, E.A., and Rougvie, A.E. (2003). The *Caenorhabditis elegans* hunchback-like gene *lin-57/hbl-1* controls developmental time and is regulated by microRNAs. *Dev. Cell* *4*, 625–637.
6. Abbott, A.L., Alvarez-Saavedra, E., Miska, E.A., Lau, N.C., Bartel, D.P., Horvitz, H.R., and Ambros, V. (2005). The *let-7* MicroRNA family members *mir-48*, *mir-84*, and *mir-241* function together to regulate developmental timing in *Caenorhabditis elegans*. *Dev. Cell* *9*, 403–414.
7. Ren, Z., and Ambros, V.R. (2015). *Caenorhabditis elegans* microRNAs of the *let-7* family act in innate immune response circuits and confer robust developmental timing against pathogen stress. *Proc. Natl. Acad. Sci. USA* *112*, E2366–E2375.
8. Frézal, L., and Félix, M.-A. (2015). *C. elegans* outside the Petri dish. *eLife* *4*, <https://doi.org/10.7554/eLife.05849>.
9. Hu, P.J. (2007). Dauer. In *WormBook*, D.L. Riddle, ed. (WormBook). <https://doi.org/10.1895/wormbook.1.144.1>.
10. Fielenbach, N., and Antebi, A. (2008). *C. elegans* dauer formation and the molecular basis of plasticity. *Genes Dev.* *22*, 2149–2165.
11. Liu, Z., and Ambros, V. (1991). Alternative temporal control systems for hypodermal cell differentiation in *Caenorhabditis elegans*. *Nature* *350*, 162–165.
12. Euling, S., and Ambros, V. (1996). Reversal of cell fate determination in *Caenorhabditis elegans* vulval development. *Development* *122*, 2507–2515.
13. Karp, X., and Ambros, V. (2012). Dauer larva quiescence alters the circuitry of microRNA pathways regulating cell fate progression in *C. elegans*. *Development* *139*, 2177–2186.
14. Golden, J.W., and Riddle, D.L. (1984). The *Caenorhabditis elegans* dauer larva: developmental effects of pheromone, food, and temperature. *Dev. Biol.* *102*, 368–378.
15. Avery, L. (2014). A model of the effect of uncertainty on the *C. elegans* L2/L2d decision. *PLoS ONE* *9*, e100580.
16. Hammell, C.M., Karp, X., and Ambros, V. (2009). A feedback circuit involving *let-7*-family miRNAs and DAF-12 integrates environmental signals and developmental timing in *Caenorhabditis elegans*. *Proc. Natl. Acad. Sci. USA* *106*, 18668–18673.
17. Butcher, R.A., Ragains, J.R., Kim, E., and Clardy, J. (2008). A potent dauer pheromone component in *Caenorhabditis elegans* that acts synergistically with other components. *Proc. Natl. Acad. Sci. USA* *105*, 14288–14292.
18. Motola, D.L., Cummins, C.L., Rottiers, V., Sharma, K.K., Li, T., Li, Y., Suino-Powell, K., Xu, H.E., Auchus, R.J., Antebi, A., and Mangelsdorf, D.J. (2006). Identification of ligands for DAF-12 that govern dauer formation and reproduction in *C. elegans*. *Cell* *124*, 1209–1223.
19. Antebi, A., Yeh, W.H., Tait, D., Hedgecock, E.M., and Riddle, D.L. (2000). *daf-12* encodes a nuclear receptor that regulates the dauer diapause and developmental age in *C. elegans*. *Genes Dev.* *14*, 1512–1527.
20. Swanson, M.M., and Riddle, D.L. (1981). Critical periods in the development of the *Caenorhabditis elegans* dauer larva. *Dev. Biol.* *84*, 27–40.
21. Butcher, R.A., Fujita, M., Schroeder, F.C., and Clardy, J. (2007). Small-molecule pheromones that control dauer development in *Caenorhabditis elegans*. *Nat. Chem. Biol.* *3*, 420–422.

22. Ren, P., Lim, C.S., Johnsen, R., Albert, P.S., Pilgrim, D., and Riddle, D.L. (1996). Control of *C. elegans* larval development by neuronal expression of a TGF-beta homolog. *Science* *274*, 1389–1391.
23. Kim, K., Sato, K., Shibuya, M., Zeiger, D.M., Butcher, R.A., Ragains, J.R., Clardy, J., Touhara, K., and Sengupta, P. (2009). Two chemoreceptors mediate developmental effects of dauer pheromone in *C. elegans*. *Science* *326*, 994–998.
24. McGrath, P.T., Xu, Y., Ailion, M., Garrison, J.L., Butcher, R.A., and Bargmann, C.J. (2011). Parallel evolution of domesticated *Caenorhabditis* species targets pheromone receptor genes. *Nature* *477*, 321–325.
25. Park, D., O'Doherty, I., Somvanshi, R.K., Bethke, A., Schroeder, F.C., Kumar, U., and Riddle, D.L. (2012). Interaction of structure-specific and promiscuous G-protein-coupled receptors mediates small-molecule signaling in *Caenorhabditis elegans*. *Proc. Natl. Acad. Sci. USA* *109*, 9917–9922.
26. Kimura, K.D., Tissenbaum, H.A., Liu, Y., and Ruvkun, G. (1997). *daf-2*, an insulin receptor-like gene that regulates longevity and diapause in *Caenorhabditis elegans*. *Science* *277*, 942–946.
27. Patterson, G.I., Kowalik, A., Wong, A., Liu, Y., and Ruvkun, G. (1997). The DAF-3 Smad protein antagonizes TGF-beta-related receptor signaling in the *Caenorhabditis elegans* dauer pathway. *Genes Dev.* *11*, 2679–2690.
28. Ogg, S., Paradis, S., Gottlieb, S., Patterson, G.I., Lee, L., Tissenbaum, H.A., and Ruvkun, G. (1997). The Fork head transcription factor DAF-16 transduces insulin-like metabolic and longevity signals in *C. elegans*. *Nature* *389*, 994–999.
29. Ludewig, A.H., Kober-Eisermann, C., Weitzel, C., Bethke, A., Neubert, K., Gerisch, B., Hutter, H., and Antebi, A. (2004). A novel nuclear receptor/coregulator complex controls *C. elegans* lipid metabolism, larval development, and aging. *Genes Dev.* *18*, 2120–2133.
30. Hammell, C.M., Lubin, I., Boag, P.R., Blackwell, T.K., and Ambros, V. (2009). *nhl-2* Modulates microRNA activity in *Caenorhabditis elegans*. *Cell* *136*, 926–938.
31. Pepper, A.S.-R., McCane, J.E., Kemper, K., Yeung, D.A., Lee, R.C., Ambros, V., and Moss, E.G. (2004). The *C. elegans* heterochronic gene *lin-46* affects developmental timing at two larval stages and encodes a relative of the scaffolding protein gephyrin. *Development* *131*, 2049–2059.
32. Bethke, A., Fielenbach, N., Wang, Z., Mangelsdorf, D.J., and Antebi, A. (2009). Nuclear hormone receptor regulation of microRNAs controls developmental progression. *Science* *324*, 95–98.
33. Huang, X., Zhang, H., and Zhang, H. (2011). The zinc-finger protein SEA-2 regulates larval developmental timing and adult lifespan in *C. elegans*. *Development* *138*, 2059–2068.
34. Aprison, E.Z., and Ruvinsky, I. (2016). Sexually antagonistic male signals manipulate germline and soma of *C. elegans* hermaphrodites. *Curr. Biol.* *26*, 2827–2833.
35. Ludewig, A.H., Gimond, C., Judkins, J.C., Thornton, S., Pulido, D.C., Micikas, R.J., Döring, F., Antebi, A., Braendle, C., and Schroeder, F.C. (2017). Larval crowding accelerates *C. elegans* development and reduces lifespan. *PLoS Genet.* *13*, e1006717.
36. MacNeil, L.T., Watson, E., Arda, H.E., Zhu, L.J., and Walhout, A.J.M. (2013). Diet-induced developmental acceleration independent of TOR and insulin in *C. elegans*. *Cell* *153*, 240–252.
37. Schindler, A.J., Baugh, L.R., and Sherwood, D.R. (2014). Identification of late larval stage developmental checkpoints in *Caenorhabditis elegans* regulated by insulin/IGF and steroid hormone signaling pathways. *PLoS Genet.* *10*, e1004426.
38. Kiontke, K., and Fitch, D.H.A. (2010). Phenotypic plasticity: different teeth for different feasts. *Curr. Biol.* *20*, R710–R712.
39. Susoy, V., Herrmann, M., Kanzaki, N., Kruger, M., Nguyen, C.N., Rödelberger, C., Röseler, W., Weiler, C., Giblin-Davis, R.M., Ragsdale, E.J., and Sommer, R.J. (2016). Large-scale diversification without genetic isolation in nematode symbionts of figs. *Sci. Adv.* *2*, e1501031.
40. Simpson, S.J., Sword, G.A., and Lo, N. (2011). Polyphenism in insects. *Curr. Biol.* *21*, R738–R749.
41. Bindels, D.S., Haarbosch, L., van Weeren, L., Postma, M., Wiese, K.E., Mastop, M., Aumonier, S., Gotthard, G., Royant, A., Hink, M.A., and Gadella, T.W., Jr. (2017). mScarlet: a bright monomeric red fluorescent protein for cellular imaging. *Nat. Methods* *14*, 53–56.
42. Arribere, J.A., Bell, R.T., Fu, B.X.H., Artilles, K.L., Hartman, P.S., and Fire, A.Z. (2014). Efficient marker-free recovery of custom genetic modifications with CRISPR/Cas9 in *Caenorhabditis elegans*. *Genetics* *198*, 837–846.
43. Kim, H., Ishidate, T., Ghanta, K.S., Seth, M., Conte, D., Jr., Shirayama, M., and Mello, C.C. (2014). A co-CRISPR strategy for efficient genome editing in *Caenorhabditis elegans*. *Genetics* *197*, 1069–1080.
44. Chen, B., Gilbert, L.A., Cimini, B.A., Schnitzbauer, J., Zhang, W., Li, G.-W., Park, J., Blackburn, E.H., Weissman, J.S., Qi, L.S., and Huang, B. (2013). Dynamic imaging of genomic loci in living human cells by an optimized CRISPR/Cas system. *Cell* *155*, 1479–1491.
45. Ward, J.D. (2015). Rapid and precise engineering of the *Caenorhabditis elegans* genome with lethal mutation co-conversion and inactivation of NHEJ repair. *Genetics* *199*, 363–377.
46. El Mouridi, S., Lecroisey, C., Tardy, P., Mercier, M., Leclercq-Blondel, A., Zariohi, N., and Boulin, T. (2017). Reliable CRISPR/Cas9 genome engineering in *Caenorhabditis elegans* using a single efficient sgRNA and an easily recognizable phenotype. *G3 (Bethesda)* *7*, 1429–1437.

STAR★METHODS

KEY RESOURCES TABLE

REAGENT or RESOURCE	SOURCE	IDENTIFIER
Bacterial and Virus Strains		
<i>E. Coli</i> : OP50	Caenorhabditis Genetics Center (CGC)	N/A
<i>E. Coli</i> : HB101	Caenorhabditis Genetics Center (CGC)	N/A
Chemicals, Peptides, and Recombinant Proteins		
Ascr#2 (C6; daumone-2)	Schroeder Laboratory (Cornell)	CAS: 946524-24-9
Ascr#3 (C9; daumone-3)	Schroeder Laboratory (Cornell)	CAS: 946524-26-1
Ascr#5 (C3)	Schroeder Laboratory (Cornell)	CAS: 1086696-26-5
Δ4-dafachronic acid (DA)	Cayman Chemical, item no. 14100	CAS: 23017-97-2
Critical Commercial Assays		
Real-time-PCR-based TaqMan for <i>C. elegans</i> microRNAs	Applied Biosystems	N/A
Experimental Models: Organisms/Strains		
<i>C. elegans</i> : Strain VT1367: <i>mals105[pCol-19::gfp]</i> V	Ambros Laboratory	VT1367
<i>C. elegans</i> : Strain VT1453: <i>mir-48 mir-241(nDf51) mals105 V; mir-84(n4037) X</i>	Ambros Laboratory	VT1453
<i>C. elegans</i> : Strain VT791: <i>mals105 V; daf-12(rh61) X</i>	Ambros Laboratory	VT791
<i>C. elegans</i> : Strain VT2962: <i>daf-7(e1372) III; mals105 V; daf-12(rh61) X</i>	This paper	VT2962
<i>C. elegans</i> : Strain VT3568: <i>daf-2(e1370) III; mals105 V; daf-12(rh61) X</i>	This paper	VT3568
<i>C. elegans</i> : Strain VT3135: <i>mals105 V; srg-36srg-37(kyIR95) daf-12(rh61) X</i>	This paper	VT3135
<i>C. elegans</i> : Strain VT2972: <i>mals105 V; daf-3(mgDf90) daf-12(rh61) X</i>	This paper	VT2972
<i>C. elegans</i> : Strain VT1308: <i>daf-7(e1372) III; mals105 V</i>	Ambros Laboratory	VT1308
<i>C. elegans</i> : Strain VT1755: <i>mals105 V; daf-3(mgDf90) X</i>	Ambros Laboratory	VT1755
<i>C. elegans</i> : Strain VT1747: <i>daf-7(e1372) III; mals105 V; daf-3(mgDf90) X</i>	Ambros Laboratory	VT1747
<i>C. elegans</i> : Strain VT2984: <i>daf-7(e1372) III; mals105 V; daf-3(mgDf90) daf-12(rh61) X</i>	This paper	VT2984
<i>C. elegans</i> : Strain VT1776: <i>daf-2(e1370) III; mals105 V</i>	Ambros Laboratory	VT1776
<i>C. elegans</i> : Strain VT3566: <i>daf-16(mgDf50) I; mals105 V</i>	This paper	VT3566
<i>C. elegans</i> : Strain VT3567: <i>daf-16(mgDf50) I; daf-2(e1370) III; mals105 V</i>	This paper	VT3567
<i>C. elegans</i> : Strain VT3569: <i>daf-16(mgDf50) I; mals105 V; daf-12(rh61) X</i>	This paper	VT3569
<i>C. elegans</i> : Strain VT3570: <i>daf-16(mgDf50) I; daf-2(e1370) III; mals105 V; daf-12(rh61) X</i>	This paper	VT3570
<i>C. elegans</i> : Strain VT3682: <i>daf-16(mgDf90) I; daf-7(e1372) III; mals105 V</i>	This paper	VT3682
<i>C. elegans</i> : Strain VT3681: <i>daf-2(e1370) III; mals105 V; daf-3(mgDf90) X</i>	This paper	VT3681
<i>C. elegans</i> : Strain VT3684: <i>daf-16(mgDf90) I; daf-7(e1372) III; mals105 V; daf-12(rh61) X</i>	This paper	VT3684
<i>C. elegans</i> : Strain VT3683: <i>daf-2(e1370) III; mals105 V; daf-3(mgDf90) daf-12(rh61) X</i>	This paper	VT3683
<i>C. elegans</i> : Strain VT2952: <i>mals105 V; daf-9(m540) daf-12(rh61) X</i>	This paper	VT2952
<i>C. elegans</i> : Strain VT3061: <i>wls51[pScm::gfp] V; daf-12(rh61rh411) X</i>	This paper	VT3061
<i>C. elegans</i> : Strain VT3057: <i>din-1(dh127) II; mir-48 mir-241(nDf51) mals105 V</i>	This paper	VT3057
<i>C. elegans</i> : <i>daf-12(rh61) hbl-1(ma430[hbl-1::mScarlet-I]) X</i>	This paper	VT3894
<i>C. elegans</i> : <i>daf-7(e1372) III; daf-12(rh61) hbl-1(ma430[hbl-1::mScarlet-I]) X</i>	This paper	VT3895
<i>C. elegans</i> : Strain VT2086: <i>lin-46(ma164) mals105 V; mir-84(n4037) X</i>	Ambros Laboratory	VT2086
<i>C. elegans</i> : Strain VT1065: <i>lin-4(e912); lin-14(n179) mir-84(n4037) X</i>	Ambros Laboratory	VT1065
<i>C. elegans</i> : Strain VT3030: <i>nhl-2(ok818) III; mals105 V; daf-12(rh61) X</i>	This paper	VT3030
<i>C. elegans</i> : Strain VT3751: <i>mals105[pCol-19::gfp] V; hbl-1(ma430[hbl-1::mScarlet-II]) X</i>	This paper	VT3571
<i>C. elegans</i> : Strain VT3893: <i>daf-7(e1372) III; hbl-1(ma430[hbl-1::mScarlet-II]) X</i>	This paper	VT3893

(Continued on next page)

Continued

REAGENT or RESOURCE	SOURCE	IDENTIFIER
Recombinant DNA		
Plasmid: pOI191. Worm mScarlet from pSEM91 is converted to mScarlet-I [41] by introducing the T74I (ACC to AtC) substitution (and subcloned to generate an HR template for tagging of <i>hbl-1</i>).	This paper	pOI191
Plasmid: pOI83. pRB1017 [42] tracr sequence is modified to the more efficient (F+E) form	This paper	pOI83
Plasmid: pOI89. <i>hbl-1</i> sgRNA for C-terminal tagging of <i>hbl-1</i> cloned into pOI83	This paper	pOI89
Plasmid: pOI91. unc-22 sgRNA [43] cloned into pOI83	This paper	pOI91
Software and Algorithms		
GraphPad Prism 8	GraphPad Software Inc. (https://www.graphpad.com/scientific-software/prism/)	RRID:SCR_002798
ZEN (blue edition)	Carl Zeiss Microscopy. (https://www.zeiss.com/microscopy/us/products/microscope-software/zen.html)	RRID:SCR_013672
ImageJ - Fiji	Open Source: (https://fiji.sc/)	RRID:SCR_002285

CONTACT FOR REAGENT AND RESOURCE SHARING

Further information and requests for reagents should be directed to and will be fulfilled by the Lead Contact, Victor Ambros, (victor.ambros@umassmed.edu).

EXPERIMENTAL MODEL AND SUBJECT DETAILS***C. elegans* culture conditions**

C. elegans strains used in this study and corresponding figures in the paper are listed in [Table S1](#). All *C. elegans* strains used in this study, which include new compound strains and new alleles generated in this paper, are also listed in the [Key Resources Table](#). *C. elegans* strains were maintained at 20°C on nematode growth media (NGM) and fed with the *E. coli* HB101 strain (See [Key Resources Table](#)).

METHOD DETAILS**Dauer and L2d-inducing plates**

For experiments involving the administration of ascarosides and/or DA, we adopted the protocol described by Butcher *et al.* [17] with modifications. Namely, *C. elegans* was fed with the *E. coli* OP50 strain on plates containing 3 mL of 1% agarose (SeaKem® LE agarose, Cat#50004) with nematode growth media (NGM) without peptone. Synthetic ascarosides (kindly provided by the labs of Frank Schroeder and Jagan Srinivasan) were dissolved in ethanol (stock concentrations: ascr#2 5.69 mM, ascr#3 3.81 mM, and ascr#5 4.09 mM) and added to the melted agarose prior to plate-pouring to achieve the desired final concentration (3 μM, if not specified) (See [Key Resources Table](#)). Plates were seeded the next day with *E. coli* strain OP50 as follows: OP50 was grown in liquid Luria Broth (LB) media until the culture reached OD₆₀₀ = 0.6-0.7. Then, the bacterial culture was pelleted by spinning at 3500 rpm for 10 min. The pellet was washed twice with a volume of sterile water equal to the LB culture volume. Finally, the pellet was resuspended in a volume of sterile water equal to one-fifth of the initial LB culture volume. 50 μLs of this washed and 5x concentrated OP50 culture were used to seed ascaroside plates. To prepare ascaroside plates also containing Δ4-dafachronic acid (DA; 1 mg of DA dissolved in ethanol, see [Key Resources Table](#)) 50 μL of water containing DA at specified concentrations was added onto the lawn of bacteria.

Analysis of extra seam cell phenotypes

Gravid adult animals were washed off from NGM plates and collected in 2 mL of water. 0.84 mL of freshly prepared 2:1 mixture of bleach (6% sodium hypochlorite, Fisher Chemical SS2901) and 5N sodium hydroxide (prepared by dissolving Fisher S318500 in distilled water) was added onto the worms in 2 mL of water. Worms were incubated in this solution containing bleach and sodium hydroxide for 3 min. To pellet the released eggs, 8 mLs of water was added, and the tube was spun for 20 s at 600 x g. The supernatant is carefully removed and the pelleted eggs were washed three times with 10 mL of sterile M9 buffer. Eggs in M9 buffer were pipetted on control or treatment plates and cultured at 20°C (unless otherwise specified) until they reached the adult stage. The worms were scored at the young adult stage for the number of seam cells using fluorescence microscopy with the help of the

mals105 [pCol-19::gfp] transgene that marks the lateral hypodermal cell nuclei or the *wls51 [pScm::gfp]* transgene that marks the seam cell nuclei.

TaqMan assays for microRNA quantification

Synchronized L1 larvae of *daf-12(rh61)* were raised on control or *ascr#2-3-5* plates at 20°C. Larvae that reached the L2/L2d-to-L3 molt were identified and picked under a dissecting microscope and collected in M9 media within two hours. For each experimental condition, three biological samples were collected, containing approximately 200 larvae per sample. Collected worms were snap-frozen and kept at –80°C until RNA extraction. RNA was extracted using the Trizol reagent (Invitrogen).

Two microliters of 30 ng/μL RNA samples were used for reverse transcription, and multiplex miR-Taqman reactions were carried out according to the manufacturer's instructions, and using an ABI 7900-HT Fast-Real Time PCR System (See [Key Resources Table](#)). MicroRNAs were assayed in three technical replicates for each biological sample. Five highly expressed microRNAs that have not been reported to be environmentally regulated (*mir-1*, *lin-4*, *mir-52*, *mir-53*, and *mir-58*), were used as a control microRNA set. The average CT of the control microRNA set was used to normalize the CTs obtained from *let-7* family microRNAs.

Tagging of *hbl-1* at its endogenous locus

A mixture of plasmids encoding SpCas9 (pOI90, 70 ng/μL), and single guide RNAs (sgRNAs) targeting the site of interest (pOI89, 20 ng/μL) and the *unc-22* gene (pOI91, 10 ng/μL) as co-CRISPR marker [43], a donor plasmid (pOI191, 20 ng/μL) containing the mScarlet-I sequence [41] flanked by homology arms, and a *rol-6(su1006)* containing plasmid (pOI124, 50 ng/μL) as co-injection marker was injected into the germlines of ten young adult worms. F1 roller and/or twitcher animals (around 200 worms) were cloned and screened by PCR amplification (Primers 12&15; [Table S2](#)) for the presence of the expected homologous recombination (HR) product. F2 progeny of F1 clones positive for the HR-specific PCR amplification product were screened for homozygous HR edits by PCR amplification of the locus using primers that flanked the HR arms used in the donor plasmid (Primers 15&16; [Table S2](#)). Finally, the genomic locus spanning the HR arms and mScarlet-I DNA was sequenced using Sanger sequencing. A single worm with a precise HR edited locus was cloned and backcrossed twice before used in the experiments. This HR edited allele, which contains a linker and the mScarlet-I sequence integrated in-frame with *hbl-1* (see [Methods S1](#)), is named as *ma430 [hbl-1::mScarlet-I]*.

Plasmid DNA purification and microinjection of worms

Plasmid DNA for tagging *hbl-1* was purified using the ZR Plasmid Miniprep Kit (Zymo Research, Cat#: 11-308AC) with a modified protocol which includes a phenol:chloroform (Phenol:ChCl3::IAA, pH = 7.9, Ambion, Cat#AM9730) extraction step before loading the samples onto the columns. First, 600 μLs of the bacterial supernatant (Step 5 of the kit's protocol) was mixed with an equal volume of phenol:chloroform and vortexed for 10 s. Then, this mixture was centrifuged at 16,000xg for 5 min and 500 μLs of the aqueous (top, transparent) layer was transferred onto the columns. The plasmid DNA on the columns were washed with both endo-free wash and wash buffers as described in the kit's protocol, and eluted with distilled water. Plasmid DNA was mixed at the final concentrations listed above for each plasmid in 20 μL of water. 3 μL of this injection mix was loaded into a glass injection needle using a microloader pipette tip (Eppendorf, 5242956003). Glass injection needles were pulled using a KOPF vertical pipette puller (model 720) and capillary glass tubes (FHC, Inc., borosil 30-30-0). Worms were immobilized on 2% agarose pads (by gently pressing the worms with a worm pick toward the agarose surface) covered with a drop of oil (Halocarbon, CAS#9002-83-9). Agarose pads were previously prepared by spreading a drop (~50-100 μLs) of 2% agarose (in water) between two cover slides (e.g., Fisherbrand 12-544E, 24X500-1.5). The immobilized worms were injected under a Zeiss Axiovert 35 inverted microscope equipped with a Leitz mechanical micromanipulator. Injected worms were washed off from agarose pads and transferred to NGM plates in M9 media using a P200 micropipette. Injected worms (P0) were cultured at 25°C in separate NGM plates for 2-3 days before F1 twitchers/rollers were cloned for culturing before genotyping.

Cloning of sgRNA plasmids

All plasmids in the injection mix had the same plasmid backbone which was derived from pRB1017 [42]. sgRNA encoding plasmids were derived from pRB1017 (first to generate pOI83) by modifying the *tracr* encoding sequence to (F+E) form of the *tracr* [44] (using the Q5 Site-Directed Mutagenesis kit, NEB Cat#E0554, and Primers 1&2; [Table S2](#)), which was reported to increase the CRISPR efficiency in *C. elegans* [45]. pOI89 and pOI91 sgRNA encoding plasmids were generated by cloning annealed primer pairs into the Bsal cloning site of pOI83 (Primers 3-6; [Table S2](#)).

Cloning of pOI191 HR template plasmid

The Golden Gate Assembly Kit (NEB Cat#E1600) is used to fuse two PCR fragments: *mScarlet* (PCR amplified from pSEM91 [46] using primers 7&8 in [Table S2](#)) and a DNA fragment containing left and right HR arms fused to the pRB1017 plasmid backbone (PCR amplified from pOI115 using primers 9&10 in [Table S2](#), which was previously generated by assembling four PCR fragments containing a left HR arm, a GFP, a right HR arm, and the backbone of pRB1017). Single colony purified plasmid DNA was used to identify colonies containing the precise assembly of the HR arms and mScarlet. pOI191 was derived from this mScarlet clone (pOI186) by mutating a single nucleotide to convert mScarlet to mScarlet-I using the Q5 Site-Directed Mutagenesis kit (NEB Cat#E0554 and Primers 11&12; [Table S2](#)).

Microscopy imaging of *C. elegans* larva

All DIC and fluorescent images are obtained using a ZEISS Imager Z1 equipped with ZEISS AxioCam 503 mono camera, and the ZEN Blue software (See [Key Resources Table](#)). Prior to imaging, worms were anesthetized with 0.2 mM levamisole in M9 buffer and mounted on 2% agarose pads. To be able to compare fluorescent signal intensities across different genetic backgrounds or larval stages, images of all larvae were taken using the same microscopy setting. These images were then stitched together (e.g., [Figure 4A](#)) using the ImageJ Fiji software and the brightness and contrast of the montaged images were adjusted to enhance the visualization of the fluorescent signal.

QUANTIFICATION AND STATISTICAL ANALYSIS

Each circle on the genotype versus number of seam cells plots shows the observed number of seam cells on one side of a single young adult worm. ≥ 20 worms for each genotype or condition are analyzed and the average number of seam cells are denoted by lateral bars in the genotype versus number of seam cell plots. The Student's *t* test is used to calculate statistical significance when comparing different genotypes or conditions. The GraphPad Prism 8 software (See [Key Resources Table](#)) is used to plot the graphs and for statistical analysis.

Current Biology, Volume 29

Supplemental Information

**Pheromones and Nutritional Signals Regulate
the Developmental Reliance on *let-7*
Family MicroRNAs in *C. elegans***

Orkan Ilbay and Victor Ambros

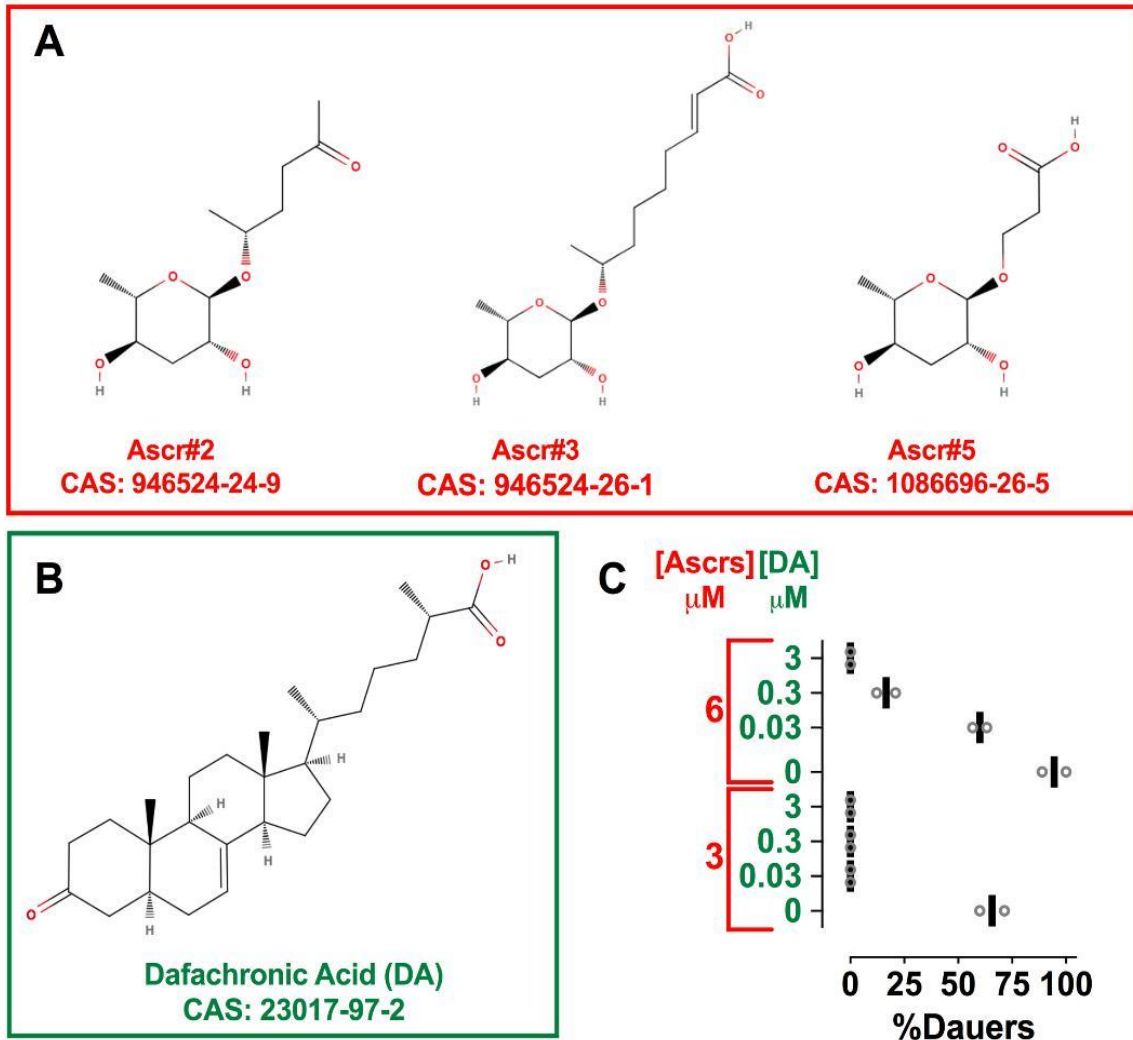


Figure S1. Chemicals and conditions used to obtain worm populations developing continuously through L2d trajectory. Related to Figure 2.

(A-B) Molecular structures (using www.molview.org), names, and CAS numbers of the chemicals used in the ascaroside (dauer-inducing), and ascaroside plus dafachronic acid (both dauer-inducing and dauer commitment inhibiting) plates.

(C) Two different concentrations of Ascrs assayed in combination with four different concentrations of dafachronic acid (DA) to determine conditions that prevent dauer formation in the presence of ascarosides. Percent dauer formation in the presence of different combinations of ascarosides (Ascrs: equimolar mixture of ascr#2, ascr#3, and ascr#5) and DA are plotted. DA inhibits dauer commitment but not L2d, which is evident by slowing of larval development. The combination of 3 μM of Ascrs and 0.03 μM DA was used as the L2d-inducing (Ascrs+DA) condition to test the effect of the L2d trajectory on the number of seam cells in wild-type and *mir-48/84/241* animals (Figure 2).

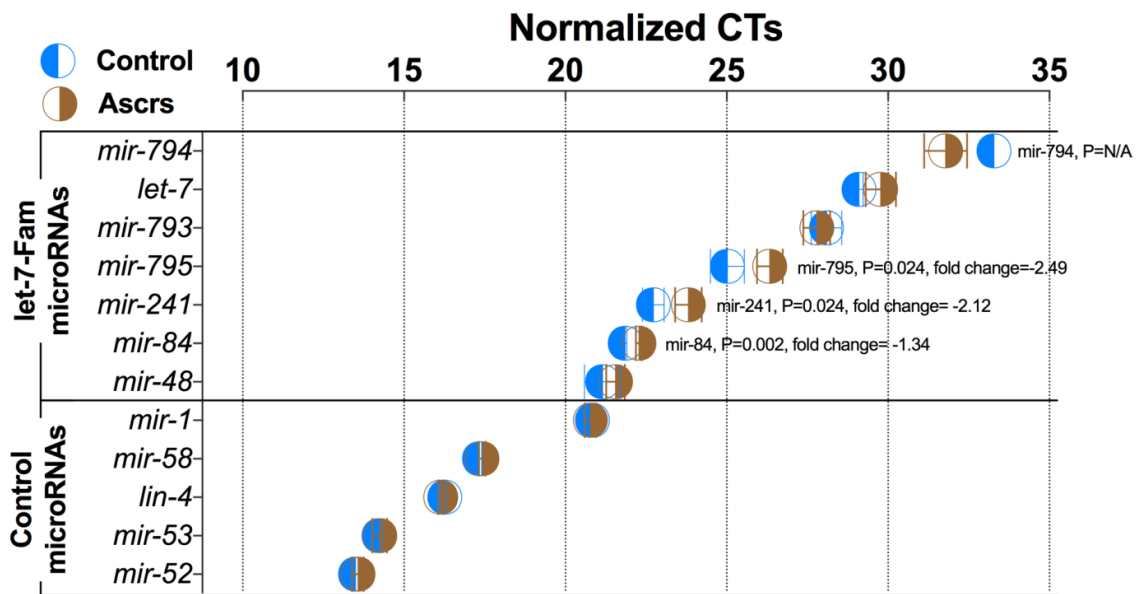


Figure S2. Ascarosides do not result in an increase in *let-7* family levels in *daf-12(rh61)* background. Related to Figure 2.

let-7 family microRNAs in L2-to-L3 (control) vs. L2d-to-L3 (Ascros) molting larvae of the *daf-12(rh61)* mutant were quantified using Taqman assays as described in the STAR methods. MicroRNAs that are highly expressed and not environmentally regulated were used as the normalization set (Control MicroRNAs). The expression levels of three *let-7* family microRNAs (*mir-84*, *mir-241*, *mir-795*) were slightly but statistically significantly reduced in the presence of ascarosides (L2d-to-L3 molt). This reduction of *let-7* family levels is in contrast with the observed suppression of retarded heterochronic phenotypes of *daf-12(rh61)* in the presence of ascarosides. The lack of an upregulation of *let-7* family microRNAs in the presence of ascarosides is in line with the idea that an alternative, *let-7*-independent, mechanism is responsible for the ascaroside-mediated suppression of the heterochronic phenotypes. *mir-794* was not detected in two biological control samples (presumably due to low expression level); therefore, we do not know if there is a statistically significant up-regulation of *mir-794* in the presence of ascarosides.

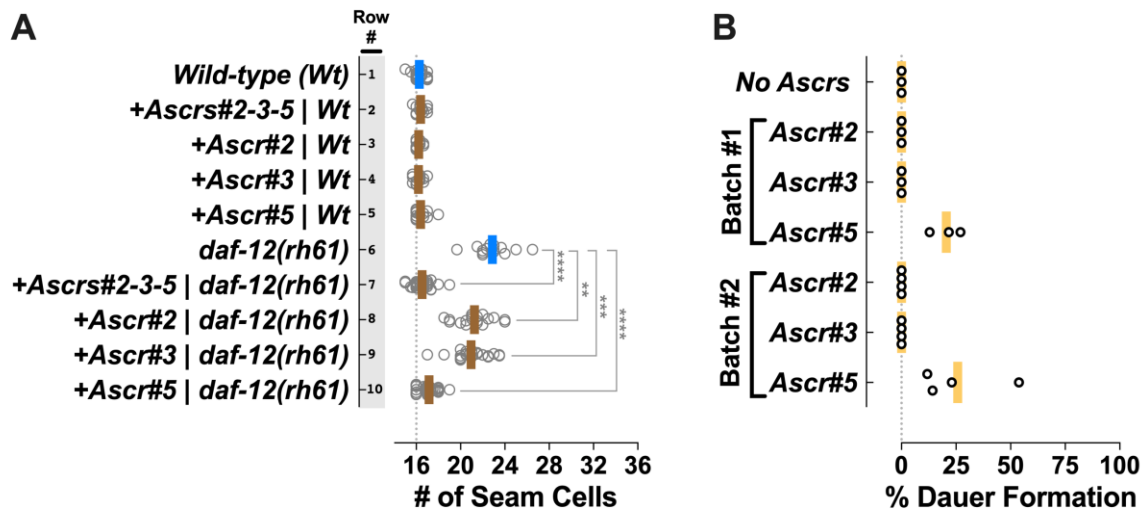


Figure S3. Testing of individual components of the pheromone cocktail for their potencies to suppress the extra seam cell phenotypes of *daf-12(rh61)* and to induce dauer formation. Related to Figure 3.

(A) Individual components of the pheromone cocktail can suppress the extra seam cell phenotypes of *daf-12(rh61)* and *ascr#5* is the most potent suppressor. Number of seam cells in young adult animals cultured under different ascaroside conditions are plotted. Each dot in the plot shows the number of seam cells of a single young adult animal, and solid lines (blue: rapid trajectory; brown: delayed [12d] trajectory) indicate the average seam cell number of the animals scored for each condition. Ascrs#2-3-5 plates contained all three ascarosides at 3 μ M final concentration of each ascaroside mixed in NGM-agarose media. Ascrs#2, Ascr#3, and Ascr#5 plates contained 3 μ M final concentration of each ascaroside mixed in NGM-agarose media. The student's t-test is used to calculate statistical significance (p): n.s. (not significant) $p > 0.05$, * $p < 0.05$, ** $p < 0.01$, *** $p < 0.001$, **** $p < 0.0001$

(B) Ascr#5 alone can induce dauer formation. At 3.3 μ M concentration, using agarose NGM plates with no peptone, seeded with washed and concentrated *E. coli* OP50 culture as described in the STAR methods, Ascr#5 alone was sufficient to induce dauer formation but not Ascr#2 or Ascr#3. We tested single ascarosides in two different batches of plates and using three or four replicates. Both experiments were performed at 20°C. Each dot on the plots shows percent dauer formation on a single plate. We maintained population sizes small (<55 worms per plate) and comparable across different Ascr plates to minimize the potential effect of the accumulation of ascarosides secreted by the worms on the plates.

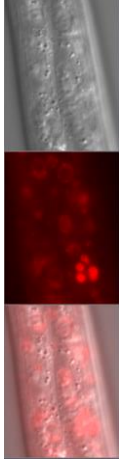

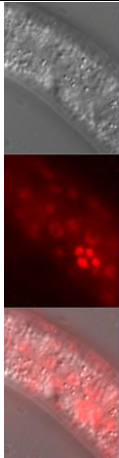
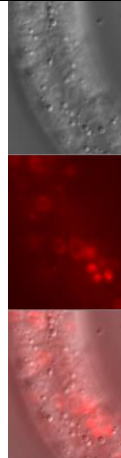

Time (Hours)	10	22	29	36	44
Genotype	<i>hbl-1(ma430[hbl-1::mScarlet-I])</i>				
Stage	L1	Late L2	L3	L4	Adult
HBL-1 Expression (# of animals scored)	Yes (10/10)	Yes (10/10)	No (0/10)	No (0/10)	No (0/10)
Example Pictures	n/a			n/a	n/a
Genotype	<i>daf-7(e1372); hbl-1(ma430[hbl-1::mScarlet-I])</i>				
Stage	L1	L2d	Late L2d	L3	L4
HBL-1 Expression (# of animals scored)	Yes (10/10)	Yes (10/10)	Yes (10/10)	No (0/10)	No (0/10)
Example Pictures	n/a				n/a

Figure S4. HBL-1 is present throughout the L2 or the lengthened L2d stage but it is absent at the post-L2 or post-L2d L3 stage. Related to Figure 5.

Endogenously tagged HBL-1 expression was examined in wild-type and *daf-7(e1372)* backgrounds at 20°C. *daf-7(e1372)* animals form dauer larvae at 25°C but they develop continuously going through L2d at 20°C. For each time point and genotype ten animals were examined. In all animals at 22 hours, also in *daf-7(e1372)* animals at 29 hours, L2 stage specific V5p cell divisions were observed to have occurred (a cluster of four small and bright nuclei in each picture), indicating that the animals were at a late phase of the L2 stage. In L2d animals the lengthening of the second larval stage appeared to occur after the execution of these L2 stage cell divisions. HBL-1 is detected in late L2 and L2d larvae but it was not detected in post-L2 and post-L2d L3 stage larvae, indicating that the duration of HBL-1 expression is lengthened as the L2 stage is lengthened during L2d, and in both post-L2 L3 and post-L2d L3 animals HBL-1 is downregulated.

Strain name	Genotype	Related figure(s)
VT1367	<i>mals105[pCol-19::gfp] V</i>	Figure 2, 3B, 3C, 3D, S1
VT1453	<i>mir-48 mir-241(nDf51) mals105 V; mir-84(n4037) X</i>	Figure 2
VT791	<i>mals105 V; daf-12(rh61) X</i>	Figure 2, 3, 4, S2, S3
VT2962	<i>daf-7(e1372) III; mals105 V; daf-12(rh61) X</i>	Figure 2, 3C, 3E
VT3568	<i>daf-2(e1370) III; mals105 V; daf-12(rh61) X</i>	Figure 2, 3D, 3E
VT3135	<i>mals105 V; srg-36srg-37(kyIR95) daf-12(rh61) X</i>	Figure 3A
VT2972	<i>mals105 V; daf-3(mgDf90) daf-12(rh61) X</i>	Figure 3B, 3C
VT1308	<i>daf-7(e1372) III; mals105 V</i>	Figure 3C
VT1755	<i>mals105 V; daf-3(mgDf90) X</i>	Figure 3C
VT1747	<i>daf-7(e1372) III; mals105 V; daf-3(mgDf90) X</i>	Figure 3C
VT2984	<i>daf-7(e1372) III; mals105 V; daf-3(mgDf90) daf-12(rh61) X</i>	Figure 3C
VT1776	<i>daf-2(e1370) III; mals105 V</i>	Figure 3D
VT3566	<i>daf-16(mgDf50) I; mals105 V</i>	Figure 3D
VT3567	<i>daf-16(mgDf50) I; daf-2(e1370) III; mals105 V</i>	Figure 3D
VT3569	<i>daf-16(mgDf50) I; mals105 V; daf-12(rh61) X</i>	Figure 3D
VT3570	<i>daf-16(mgDf50) I; daf-2(e1370) III; mals105 V; daf-12(rh61) X</i>	Figure 3D
VT3682	<i>daf-16(mgDf90) I; daf-7(e1372) III; mals105 V</i>	Figure 3E
VT3681	<i>daf-2(e1370) III; mals105 V; daf-3(mgDf90) X</i>	Figure 3E
VT3684	<i>daf-16(mgDf90) I; daf-7(e1372) III; mals105 V; daf-12(rh61) X</i>	Figure 3E
VT3683	<i>daf-2(e1370) III; mals105 V; daf-3(mgDf90) daf-12(rh61) X</i>	Figure 3E
VT2952	<i>mals105 V; daf-9(m540) daf-12(rh61) X</i>	Figure 3F
VT3061	<i>wIs51[pScm::gfp] V; daf-12(rh61rh411) X</i>	Figure 3G
VT3057	<i>din-1(dh127) II; mir-48 mir-241(nDf51) mals105 V</i>	Figure 3H
VT3894	<i>daf-12(rh61) hbl-1(ma430[hbl-1::mScarlet-I] X</i>	Figure 4A
VT3895	<i>daf-7(e1372) III; daf-12(rh61) hbl-1(ma430[hbl-1::mScarlet-I] X</i>	Figure 4A
VT2086	<i>lin-46(ma164) mals105 V; mir-84(n4037) X</i>	Figure 4B
VT1065	<i>lin-4(e912); lin-14(n179) mir-84(n4037) X</i>	Figure 4C
VT3030	<i>nhl-2(ok818) III; mals105 V; daf-12(rh61) X</i>	Figure 4D
VT3751	<i>mals105 V; hbl-1(ma430[hbl-1::mScarlet-I] X</i>	Figure S4
VT3893	<i>daf-7(e1372) III; hbl-1(ma430[hbl-1::mScarlet-I] X</i>	Figure S4

Table S1. *C. elegans* strains used in this study. Related to Figure 2, 3, 4 and 5.

All gene, allele, and transgene names, and chromosome numbers are italicized (Genotype column). *mals105* and *wIs51* are integrated extrachromosomal arrays expressing *pCol-19::gfp* and *pScm::gfp* to mark hypodermal cells of adult stage animals and hypodermal seam cells at all stages, respectively. All figures related to each strain are listed in the related figures column.

Primer #	Primer name	Primer Sequence (5' to 3')	Used for
1	Forward (pOI301)	gtttaagagctatgctggaacagcatagcaagttaaataaggctagtcgg	To generate pOI83 by modifying the tracr sequence of pRB1017
2	Reverse (pOI302)	agagaccgagtagcgggttctc	
3	Forward (priOI316)	tctgaagccagacaccaataatg	Cloning of pOI89 – <i>hbl-1</i> (<i>sgRNA</i>)
4	Reverse (priOI317)	aaaccattattggtgtctggcttc	
5	Forward (priOI323)	tcttgaaccggtgccgaatacac	Cloning of pOI91 – <i>unc-22</i> (<i>sgRNA</i>)
6	Reverse (priOI324)	aaacgtgtattcggcaacgggttc	
			Cloning of pOI191- HR template
7	Forward (priOI670)	gaaggtctcatctggagggtgatctggagggtgatctggagggtgatctgtc agcaagggagagggcagttatc	To amplify <i>mScarlet</i> from pSEM91 and to fuse with a linker
8	Reverse (priOI671)	gaaggtctcactttagagctcgtccattcc	
9	Forward (priOI672)	gaaggtctcacaagtaatgaggacgtcctctgtaagg	To amplify a fragment containing the HR arms+ plasmid backbone from pOI115
10	Reverse (priOI673)	gaaggtctcacagattggtgtctggcttggtacat	
11	Forward (priOI705)	cccacaattcatgtacggatcccgtgccttcatcaagcaccagccg	To convert <i>mScarlet</i> to <i>mScarlet-I</i> using SDM (T74I = acc>atc)
12	Reverse (priOI706)	gagaggatgtcccaggagaat	
13	Left Arm-Forward (priOI342)	cgggaattcaaatgagcggagtaagcgt	To clone the HR arms for the assembly of pOI115 (these primers define the ends of the HR arms)
14	Right arm – Reverse (priOI343)	gccggatccaacaagtattctgggggaggt	
15	Forward (priOI262)	tcacccggagacgaggagac	Screening of F1 progeny of CRISPR mix injected P0 worms for HR (<i>hbl-1::mScarlet-I</i>) events
12	Reverse (priOI706)	gagaggatgtcccaggagaat	
15	Forward (priOI262)	tcacccggagacgaggagac	Screening of F2 progeny of F1 worms positive for HR events – these primers flank the HR arms
16	Reverse (priOI228)	aaaagagcagcagagttgg	

Table S2. Primers used in this study. Related to STAR Methods.